


Cite this: *RSC Appl. Polym.*, 2026, **4**, 502

# Unlocking high-performance capacitive energy storage: advances in polymer nanocomposite dielectrics

Tanuj Kumar,<sup>a</sup> \*<sup>a</sup> Rahul Singhal,<sup>b</sup> Ramesh Kumar,<sup>c</sup> Arunima Verma,<sup>a</sup> Priya Jasrotia,<sup>a</sup> Arun Kumar,<sup>d</sup> Rajeev Gupta,<sup>e</sup> Ajay Singh Verma,<sup>f</sup> Priyankaben Trivedi<sup>g</sup> and Manju Bala<sup>h</sup>

The dielectric properties of polymers at extreme temperatures for energy storage require significant improvement, despite their superior processability, strong dielectric breakdown strength, and great mechanical qualities. By combining the best features of polymers and ceramics, scientists have created polymer nanocomposites with enhanced dielectric properties, making them ideal for use in various applications, including aerospace, oil and gas exploration, and hybrid electric cars. Interfacial design, micro-structural engineering, and new high-dielectric filler materials are some of the important tactics and analytical models that have been developed to significantly increase the energy density of composite dielectrics. Novel designs have resulted from combining analytical models with machine learning approaches. Also covered in this study is the effect of a high-temperature implanted nanofiller on energy density in a polymer matrix. Lastly, this review summarizes the many types of dielectrics and their respective benefits, advancements, drawbacks, and limits when subjected to wide temperature ranges. An overview of the current areas where there is increasing production of energy storage devices in electric vehicles, pulsed warfare systems, and power electronics is provided to illustrate the practical uses of polymer nanocomposite dielectrics. We conclude by discussing the difficulties and potential benefits of polymer nanocomposite dielectrics in unusual scenarios.

Received 4th December 2024,  
Accepted 2nd January 2026

DOI: 10.1039/d4lp00357h

rsc.li/rscaplpolym

## 1. Introduction: advanced dielectric polymers

Numerous fields rely on dielectric materials, including micro-electronics, power electronics, power grids, healthcare, and defence. Research efforts have focused on creating better dielectrics that can store a lot of energy because of the huge demand. A considerable portion of the market is occupied by film capacitors, ceramic capacitors, and electrolytic capacitors

based on tantalum and aluminium. Ceramic capacitors are mainly used in low voltage applications, such as miniature consumer electronics, due to their high-frequency operational properties and relatively low capacitance.<sup>1</sup> However, they have many other uses as well, and there are clear problems with ceramic capacitors such as their low breakdown strength, mechanical cracking, and unreliability, particularly in big components.<sup>2,3</sup> For low-frequency applications requiring ripple current suppression, electrolytic capacitors are a good choice due to their enormous capacitance. Due to its high voltage operation, reliability, and wide capacitance range, film capacitors offer exceptional benefits. Since organic film dielectrics are both flexible and resistant to high electric fields, it is ideal for use in low-cost capacitor manufacturing processes, winding processes involving metal foil or metallization, and other applications.<sup>4</sup> The organic dielectrics used in the production of organic film capacitors typically include polystyrene (PS), polypropylene (PP), polyethylene naphthalate (PEN), polyethylene terephthalate (PET), polytetrafluoroethylene (PTFE) and polycarbonate (PC).<sup>5,6</sup> It would appear that thinner and more pliable organic films are necessary to meet the rising demand for small but highly effective electronic components. In order to realize compact capacitors with a broad range of

<sup>a</sup>Department of Physics and Astronomical Sciences, Central University of Jammu, Jammu, 181143, India. E-mail: tanuj.nsm@cuammu.ac.in

<sup>b</sup>Department of Physics, Malaviya National Institute of Technology, Jaipur, Rajasthan, 302017, India

<sup>c</sup>Department of Physics, Guru Jambheshwar University of Science and Technology, Hisar-125001, India

<sup>d</sup>Physics Department, J.C. Bose University of Science and Technology, YMCA, Faridabad-121006, India

<sup>e</sup>Department of Physics, School of Engineering Studies, University of Petroleum & Energy Studies, Dehradun 248007, India

<sup>f</sup>Division of Research & Innovation, School of Applied and Life Sciences, Uttarakhand University, Dehradun, Uttarakhand, 248007, India

<sup>g</sup>Department of Physics, H. & H.B. Kotak Institute of Science, Rajkot, Gujarat, India

<sup>h</sup>Department of Physics, Hindu College, University of Delhi, India



capacitance and voltage designs, it is becoming increasingly important to produce thin films with high dielectric constant, low dielectric loss, and high dielectric strength. This is despite the fact that most synthetic dielectric polymers are abundant in raw materials and suitable for capacitor development.<sup>7</sup> There has been a lot of focus on enhancing the electrolyte durability, safety, and energy density in lithium-ion batteries because they are one of the most popular and efficient electrochemical energy storage systems. Polymer solid electrolyte membranes or composites undergo UV-induced crosslinking to reduce crystallite formation and increase ionic conductivity, resulting in all-solid-state Li-ion batteries with superior cycling stability and Coulombic efficiency. Electrolytes based on ionic liquids created using the UV-induced free radical polymerization process or multipolymer electrolyte membranes powered by oxygen energy cathodes are also an option.<sup>8,9</sup> A solvent-free preparation procedure yields hybrid solid electrolytes, which offer a scalable solution for Li-based batteries. Achieving high density, improved safety, and excellent stability has been suggested as a means to design smart rechargeable commercial Li-based batteries and multivalent metal and metal-ion rechargeable batteries.<sup>10,11</sup> This is in line with recent advances in the field of organic and metal-organic polymer electrodes. However, the major problems with Li-based batteries are resource scarcity and the unavoidable pollution they cause. In contrast, photocatalysis is a practical energy storage technology that is often used to produce hydrogen and degrade organic pollutants. One method that has shown great effectiveness in both of these areas is the photo-assisted isoelectric point method. Nanostructured conjugated polymers are engineered through structural modifications and the incorporation of different functional moieties to provide sustainable and adaptable energy devices that go beyond solar cells.<sup>12</sup>

In response to an external electric field that is both static and oscillating, the charge carriers within a dielectric material either move about or react, which in turn causes a number of

dielectric phenomena. Simply put, a lossy dielectric phenomena characterized by an extremely high dielectric constant and dielectric loss can be caused by the slowest reaction of an interfacial polarization in a dielectric substance. For frequencies below 100 Hz, this effect can manifest in dielectric materials or capacitor components. Dipolar polarization, atomic polarization, and electronic polarization are the three basic causes of polymeric dielectric responses (Fig. 1a). Dipolar or orientation polarization is strongly related to the relaxation of electric dipoles that exhibit high dielectric constants and respond to an alternating electric field in a wide frequency range (up to  $10^5$  Hz). When the applied field is removed, the relaxation time or response frequency of the dipoles is affected by how quickly they return to their non-oriented states. As a result of nucleus displacement, atomic polarization can occur in response to alternating electric fields at frequencies as high as  $10^{13}$  Hz, which are infrared or far-infrared. Although electrons can travel at high speeds up to the ultraviolet frequency domain ( $10^{15}$  Hz), polarization causes them to slow down.<sup>13</sup> There is a strong relationship between the bandgap of dielectrics and electronic polarization, as well as dielectric response, where  $n$  is the refractive index and  $K$  is the electronic polarization dielectric constant. In contrast to ceramics with strongly correlated dipoles, such as ferroelectric ceramics, polymers display a lower dipole moment and differential correlation. The lower dielectric constant is mostly due to the dielectric polymer possessing poorer dipolar correlation and higher barriers for dipoles to spin in response to applied fields. Dielectric polymers have become indispensable in modern electrical technologies because their lightweight, flexible, and highly insulating nature enables functions that rigid inorganic dielectrics cannot easily achieve. They form the backbone of numerous capacitor systems—from compact film capacitors used in everyday electronics to high-energy-density devices that power advanced inverters, pulsed systems, and electric vehicles.<sup>14</sup> Their exceptional insulating strength also

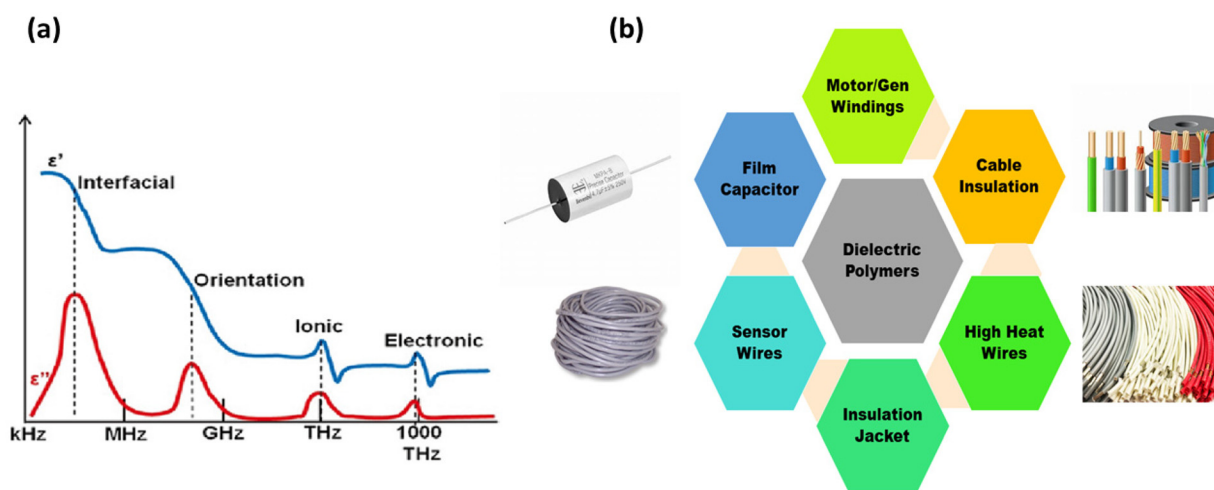


**Fig. 1** (a) Real ( $\epsilon'$ ) and imaginary parts ( $\epsilon''$ ) of the dielectric constant as a function of frequency in a polymer having interfacial, orientational, ionic, and electronic polarization adapted from ref. 15. (b) Typical applications of dielectric polymers in various electrical components and systems.



makes them essential in safeguarding electrical infrastructure, serving as protective layers in cables, motors, transformers, and high-voltage equipment. In the realm of electronics, dielectric polymers act as key components in thin-film transistors, organic circuits, flexible displays, and encapsulation layers that shield sensitive devices from environmental stress. Beyond traditional roles, they enable next-generation technologies such as soft actuators, wearable electronics, stretchable sensors, and high-temperature polymer nanocomposites for aerospace and automotive systems. This broad utility—spanning power engineering, microelectronics, and emerging flexible technologies—highlights the remarkable versatility of dielectric polymers in shaping contemporary and future electrical systems, as shown in Fig. 1b.

The energy-storage capability of a dielectric material is quantified using eqn (1), which represents the energy density stored per unit volume when an electric field is applied, as seen in the grey region of Fig. 2.<sup>16</sup> In this expression,  $E$  denotes the electric field strength and  $D$  represents the electric displacement, which is directly related to the material's polarization. The integral corresponds to the area under the  $D$ - $E$  curve, indicating the total energy stored during the charging process. This equation is crucial for evaluating the charge-discharge behavior and efficiency of dielectric materials, as it allows researchers to determine how much usable energy a material can deliver and how much is lost due to leakage or hysteresis. By applying this relation, one can compare the performance of different dielectric films, assess their suitability for high-energy-density capacitors, and optimize materials for advanced applications in power electronics, electric vehicles, and high-temperature energy-storage systems.

$$W = \int E dD \quad (1)$$

The energy density of a linear dielectric material can also be expressed using eqn (2), which provides a simplified form

for systems where the polarization response is linear with respect to the applied electric field (Fig. 2(b)).<sup>16,17</sup> In this equation,  $\epsilon_0$  is the permittivity of free space,  $\epsilon_r$  is the relative permittivity of the dielectric material, and  $E$  is the applied electric field strength. The expression shows that the stored energy density increases quadratically with the electric field and is directly proportional to the dielectric constant of the material. This formula is widely used to estimate the maximum theoretical energy storage capability of linear dielectrics such as polymer films and ceramic-based capacitors. It helps researchers quickly compare materials, optimize dielectric constants, and predict energy performance in capacitor design, making it essential in evaluating high-energy-density dielectric systems.

$$W = \frac{1}{2} \epsilon_0 \epsilon_r E^2 \quad (2)$$

Although a high electric field can be used to charge materials with a high energy density, it also causes energy loss and current leakage, which reduces the efficiency of energy storage. The material efficiency in storing energy is just as crucial as its density when it comes to real-world applications. As a percentage, the energy storage efficiency is the ratio of the density of stored energy during discharge to that while charging (eqn (3)):

$$\eta = \frac{W_d}{W_e} \quad (3)$$

whereby,  $W_e$  is the charging energy density and  $W_d$  is the discharge energy density. Increasing the energy storage efficiency of the dielectrics usually leads to less energy loss and better reliability.

Due to their capacity to combine the high electrical breakdown strength of polymer matrix materials with the high permittivity of ceramic dielectric fillers, polymer/inorganic nanoparticle nanocomposite dielectrics have garnered a lot of attention for electric energy storage applications. The improvement

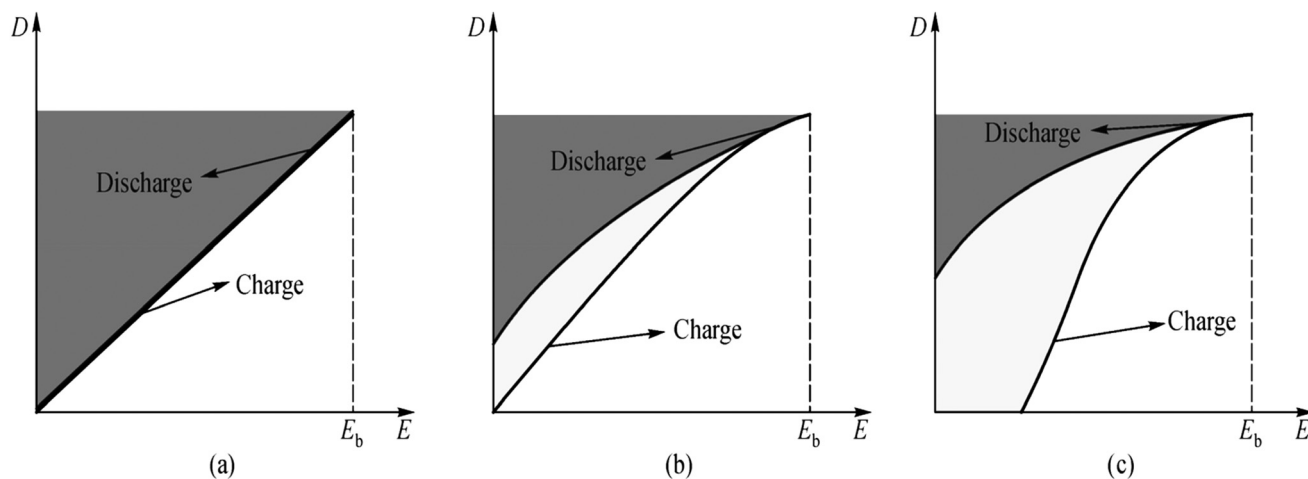


**Fig. 2** (a–c) Schematics of the three common  $D$ - $E$  curves. The black line represents the charge pathway and the discharge pathway. Here, we can see the density of charging energy in the grey area and the density of losing energy in white area. For dielectrics, the breakdown field strength is denoted by  $E_b$ , reproduced from ref. 16 with permission from Springer Nature.



in the dielectric permittivity ( $\epsilon_r$ ) typically results in a decrease in the breakdown strength ( $E_b$ ), which is a big problem with these composite dielectrics.<sup>18</sup> There are a few common reasons why the breakdown strength decreases: (a) there is a significant difference in the dielectric permittivity between the polymer matrix and inorganic ceramic fillers, which causes a local electric field distortion at the interface;<sup>19</sup> and (b) filler agglomeration and composite defects due to incompatibility between the two materials.<sup>20,21</sup> Thus, increasing the breakdown strength and dielectric permittivity of polymer composite dielectrics at the same time is still a formidable task. Recent developments in polymer nanocomposite dielectrics are covered in this review. Topics covered include extensive synthetic procedures, main techniques for improving the energy density, efficiency, and stability, and new uses for these materials. As a conclusion, this review compiles information about the various dielectrics and their advantages, disadvantages, improvements, and limitations over a wide temperature range. To show how polymer nanocomposite dielectrics are being used in electric vehicles, pulsed warfare systems, and power electronics, we will take a look at some examples of how energy storage devices are being mass-produced right now. Finally, we discuss the applications of polymer nanocomposite dielectrics, and the challenges and opportunities they present in non-standard situations.

## 2. Methods for increasing the energy storage density in capacitors

The density of energy storage is the central metric for all criteria used to estimate the efficiency of energy storage materials. In section 1, we discussed the energy density equations. From these equations, we can see that to improve the energy storage density of polymer-based materials, we can increase the dielectric constant and field strength of the materials.

### 2.1 Polymer polarity enhancement

A key strategy in unlocking the high-performance capacitive energy storage in polymer nanocomposite dielectrics lies in simultaneously leveraging organic–inorganic hybridization and polymer polarity enhancement. Organic–inorganic hybridization enables the integration of flexible polymer matrices with high-permittivity inorganic nanofillers, creating strong interfacial interactions that suppress charge injection, reduce conduction loss, and improve breakdown strength. At the same time, enhancing the intrinsic polarity of the polymer—through molecular engineering, functional group incorporation, or controlled chain orientation—significantly increases dipole density and alignment, thereby boosting dielectric permittivity and energy density without compromising stability. When these two mechanisms act synergistically, the resulting nanocomposites exhibit substantially improved charge–discharge efficiency, elevated high-temperature performance, and superior reliability under high electric fields. Together, hybrid-

ization and polarity enhancement represent a powerful design framework for next-generation polymer dielectrics capable of meeting the demands of advanced capacitive energy-storage technologies.

The high dielectric constant (about 10 at 1 kHz) of ferroelectric polymers made of polyvinylidene fluoride (PVDF) is a result of their dipolar spontaneous polarization and inherently strong polar C–F linkages.<sup>22</sup> As a result of the huge electronegativity difference between the carbon and fluorine atoms, the C–F bond has a strong dipole moment of  $6.4 \times 10^{-30}$  C m, making it a base unit with high polarity.<sup>23</sup> PVDF has a crystallinity ranging from 50% to 60%, and can crystallize into several crystal phases (*e.g.*,  $\alpha$ -,  $\beta$ -,  $\gamma$ - *etc.*). Through the co-polymerization of vinylidene fluoride with trifluoro ethylene (TrFE), chlorotrifluoroethylene (CTFE), hexafluoropropylene (HFP), and bromotrifluoroethylene (BTFE), researchers have created a series of PVDF-based binary copolymers with an increased dielectric constant.<sup>24–27</sup> P(VDF-TrFE) 18 at 1 kHz, P(VDF-CTFE) 13 at 1 kHz, P(VDF-HFP) 5.6 at 1 kHz, and P(VDF-BTFE) are all examples of PVDF-based binary copolymers with higher dielectric constants. When exposed to electrons, one of these materials, P(VDF-TrFE), takes on the properties of ferroelectric polymers. The addition of a third component, a polymer, can further improve the material dielectric constant. Several studies have shown that ternary copolymers with higher dielectric constants, like P(VDF-TrFE-CFE) (55 at 1 kHz) and P(VDF-TrFE-CTFE) (47 at 1 kHz), can be produced by adding fluorovinyl chloride (CFE) and CTFE<sup>41,42</sup> to the P(VDF-TrFE) binary copolymer.<sup>28,29</sup> Prabhune, P., *et al.*<sup>30</sup> proposed a design framework for optimizing multiple properties by tuning the design variables, including the microstructural and interface characteristics. Finally, we employed mixed-variable global sensitivity analysis to understand the complex interplay between four continuous microstructural parameters and two categorical interface choices, enabling deeper physical insights into the design of nanodielectrics.

### 2.2 Organic–inorganic hybridization

To further increase the energy storage density of polymer-based dielectrics, organic–inorganic hybridization is an additional effective method. This necessitates the incorporation of dielectric-sensitive ceramic materials, such as BaTiO<sub>3</sub> (BT), BaSrTiO<sub>3</sub>, and SrTiO<sub>3</sub>.<sup>31–34</sup> When ceramic particles are embedded into a polymer matrix, the resulting composite generally shows a dielectric constant that falls between that of the pure polymer and the ceramic filler. The final value depends on several factors, including the filler volume fraction, particle morphology, interfacial polarization, and the quality of dispersion within the polymer matrix. Past research has demonstrated that the dielectric constant is sensitive to the filler type, size and distribution. In order to get the best possible composite design, it is possible to determine the composite system's dielectric constant by applying the appropriate mathematical models. Nevertheless, extensive experimental work has shown that, in most cases, a high dielectric constant requires a substantial number of inorganic fillers. A material with a dielec-



tric constant of 100 and a filler percentage of roughly 40% was produced by Bai *et al.*<sup>35</sup> using a polymer as the basis. Composites made using polymers and high-dielectric-constant ceramics, including ferroelectric ceramics, can have a substantially lower ceramic content need due to the increased dielectric constant. In order to create ceramic polymer composites with PVDF as the matrix, Wang *et al.*<sup>36</sup> utilized Na0.35% Ba99.65%–Ti99.65%Nb0.35%O<sub>3</sub> (NNBT) as a filler. A dielectric constant of above 100 at 1 kHz and a dielectric loss of approximately 0.037 at 1 kHz were observed in PVDF-0.5NNBT with a filler content of 10 vol%, according to their data. Table 1 provides a summary of the important data.

According to research,<sup>38,39</sup> the dielectric characteristics of composites are significantly affected by the interface between the matrix and the filler. As the physical boundary between the two components, the interfacial region of a composite often exhibits characteristics that are distinct from those of either component alone. Considerations such as the component type, environmental factors, and interface strength all play a role in determining the relative size of the interface area. We may see the interface in action in two classical models: Tanaka<sup>40</sup> and Lewis.<sup>41</sup> Fig. 3(a) shows the proposed path of the leakage current along the nanoparticle interface, according to the Lewis model. This current would leak out of the inorganic particle filler and into the load system. As a result of the ionization of the functional groups on the surface of the filler particles, an equilibrium of the Fermi level or chemical potential happens. A diffusion double layer structure forms close to the interface as the charged particles readily absorb the charge in the matrix, and the composite material with electrical conductivity can be changed by modifying its interface structure. Fig. 3(b) from Tanaka's model shows the proposed three-layer division of the interfacial region between the organic matrix and the inorganic nanoparticles. These layers are the bonding layer, the constraining layer, and the loose layer. Both the interface thickness and the materials' dielectric characteristics are affected by the interaction strength between the bonding layer and the particles.

### 2.3 Methods for processing dielectric polymer films

Implementing scalability and proving the practicality of innovative dielectric films are crucial for advanced dielectric polymers to be successful in energy storage applications. Reducing thickness and size scale while expanding the length scale are obstacles that dielectric polymer film manufacturing must

overcome. Over the last 30 years, the dielectric community has developed and implemented numerous significant processing methods for the manufacturing of polymer films and composites, moving from laboratory scale to mass production, with the goal of using these materials to capacitors and dielectric films. Dielectric polymer films can be fabricated using a variety of processing techniques, with each tailored to achieve precise control over the film thickness, microstructure, and dielectric performance. Solution-based methods such as spin coating, drop casting, and blade coating are widely used for producing uniform thin films, offering excellent scalability and compatibility with nanofiller dispersion in polymer nanocomposites. Melt extrusion and hot pressing are commonly employed for thermoplastic dielectric polymers, enabling the formation of mechanically robust, large-area films without the need for solvents. Advanced techniques such as electrospinning can generate ultrathin fibrous dielectric layers with high surface area, while layer-by-layer assembly and Langmuir–Blodgett deposition allow for nanoscale control over multilayer architectures for high-performance capacitors. Additionally, chemical vapor deposition (CVD) and plasma polymerization can be used to fabricate highly pure, defect-minimized dielectric coatings. The choice of processing method plays a crucial role in determining the film's morphology, crystallinity, defect density, and ultimately its dielectric breakdown strength and energy-storage capability.

**2.3.1 Solution casting and electrospinning methods for films with carriers.** The solution casting method is favoured in dielectric polymer research due to its many advantages, including its processability, low investment requirements, ease of access, and readiness to work with polymer films ranging in thickness from 5 to 20 μm. Solvent evaporation at elevated temperatures, coating on a detachable carrier, coating with a polymer solution, and finally, removing the film from the carrier are the steps involved in solution casting. It is common practice in laboratories to use this procedure to make films of polymers or polymer nanocomposites that are appropriate for rapid dielectric evaluations. Some thermoplastic materials can also be mass-produced using this technique. Recently, Sigma Technologies developed a new method for making solution cast films that involves deposition of many layers of extremely thin polymer films in real time. The thin film of less than 500 nm thickness is created by coating the prepared dilute polymer solution onto a substrate, and then curing it with e-beam radiation. The same manufacturing room is used to

**Table 1** Volume fractions of many common ceramic fillers used to increase the composite dielectric constants, as well as the composites' own dielectric constants

S. no.	Authors	Polymer	Ceramic fillers	Filler/vol%	$\epsilon_a$	$\epsilon_b$	Ref.
1.	Hao Y., Wang X. <i>et al.</i>	P(VDF-HFP)	BT	30	~5	~20	31
2.	Lu X., Zhang L. <i>et al.</i>	P(VDF-CTFE)	BaSrTiO <sub>3</sub>	40	~13	~38	37
3.	Yao L., Pan Z. <i>et al.</i>	PVDF	SrTiO <sub>3</sub>	10	~10	~18	34
4.	Bai Y., Cheng Z. Y. <i>et al.</i>	P(VDF-TrFE)	Pb(Mg <sub>1/3</sub> Nb <sub>2/3</sub> )O <sub>3</sub> –PbTiO <sub>3</sub>	40	~18	~100	35

$\epsilon_a$  Dielectric constant of polymer;  $\epsilon_b$  Dielectric constant of filler.



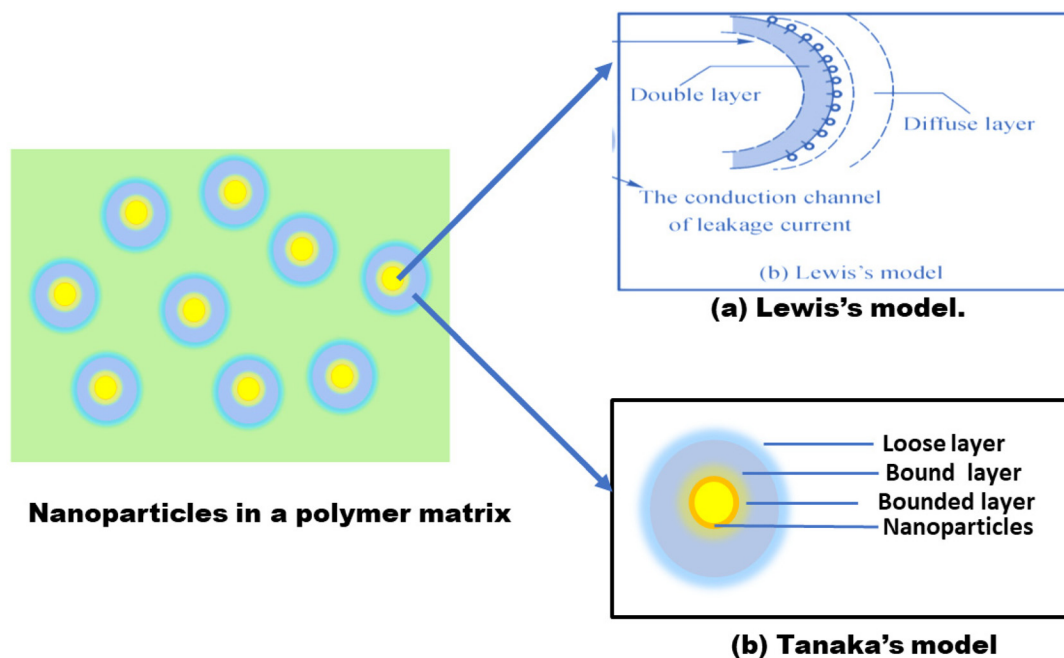


Fig. 3 Schematics of the (a) Lewis's model and (b) Tanaka's model.<sup>40,41</sup>

immediately deposit nanometre-sized aluminium electrodes through evaporation, shielding them from environmental conditions. To make a solid-state polymer-multi-layer capacitor, this alternate coating process is repeated thousands of times. There are thousands of polymer dielectric layers and aluminium electrodes in the nanolaminate, giving it a high capacitance and expansive surface area. The part is subsequently divided into separate prismatic capacitors with specific ratings, like 400 VDC, 600 VDC max, 700  $\mu\text{F}$ , 165 A, or 295 A max. Supposedly, multilayer dielectric capacitors exhibit low ESL and ESR, a wide operating temperature range of  $-40$  to  $140$   $^{\circ}\text{C}$ , and a high breakdown strength greater than  $1000$   $\text{V } \mu\text{m}^{-1}$ . The dissipation factor is less than  $0.01$  and the dielectric constant ( $k$ ) ranges from  $3.0$  to  $6.2$  for the polymer.<sup>42</sup> To create polymer composites with nanofibers, scientists create synthetic nanocomposites by manipulating the three-dimensional distribution and orientation of nanoparticles within a polymer matrix.<sup>43</sup> A polymer or precursor is dissolved or melted before being jet-spun into fibres using a powerful electric field. The procedure entails extending the filament from the cone tip and transforming the spherical droplet at the needle tip into a conical item. Additional nanometre-diameter polymer nanofibers can be manufactured<sup>44–46</sup> (Fig. 4). By compressing the fibres, polymer films can be further reinforced. Polymer products are commonly made *via* hot compression moulding, which is also a standard technique for film samples employed in research laboratories. This technique involves pressing the mold over heating plates, which allows for precise temperature and timing control. The polymer film is melted and then cooled, all while maintaining the pressure. The final products of compression molding have a high density and consistent thickness, which are benefits over other processing processes.

Regardless of whether there are neat polymers or nanocomposites, it can only handle films that are thicker than approximately  $20$   $\mu\text{m}$ . Electrospinning is a powerful technique that can create fibres with a wide range of diameters, a high specific surface area, and a consistent distribution of diameters.<sup>45</sup> Biomedical, environmental engineering, textile, and other domains can greatly benefit from this approach. It works well with roll-to-roll production methods. Furthermore, it has the potential to be a generic technology for making complicated nanostructured composites on a large scale, which is currently unattainable with conventional polymer processing methods. However, its large-scale application is limited by electro-spinning low efficiency, solvent expensive cost, and recycling complexity.

**2.3.2 Melt casting for free-standing polymer films.** The most significant fraction of products in the field of polymer processing, the most variety, high productivity, strong flexibility, wide range of uses, and more than a century of development have all gone into blow molding and melt extrusion.<sup>49</sup> The processing and fabrication of thicker films have traditionally suited blow molding. The production technique has restrictions and the materials have faults that cannot be solved. Hence, it cannot be used for thinner films.<sup>50</sup> In the 1980s, a new method for producing and processing films called extrusion emerged. One of its key components, multi-layer co-extrusion technology, allowed tape casting to become a widely used film-manufacturing and processing tool. Since then, extrusion has found its way into a variety of film packaging.<sup>51</sup> Extrusion is a process that involves plasticizing a material by heating or applying pressure. The material is then forced through molds with orifice plates, and the correct cross-section is maintained through cooling or chemical reactions.



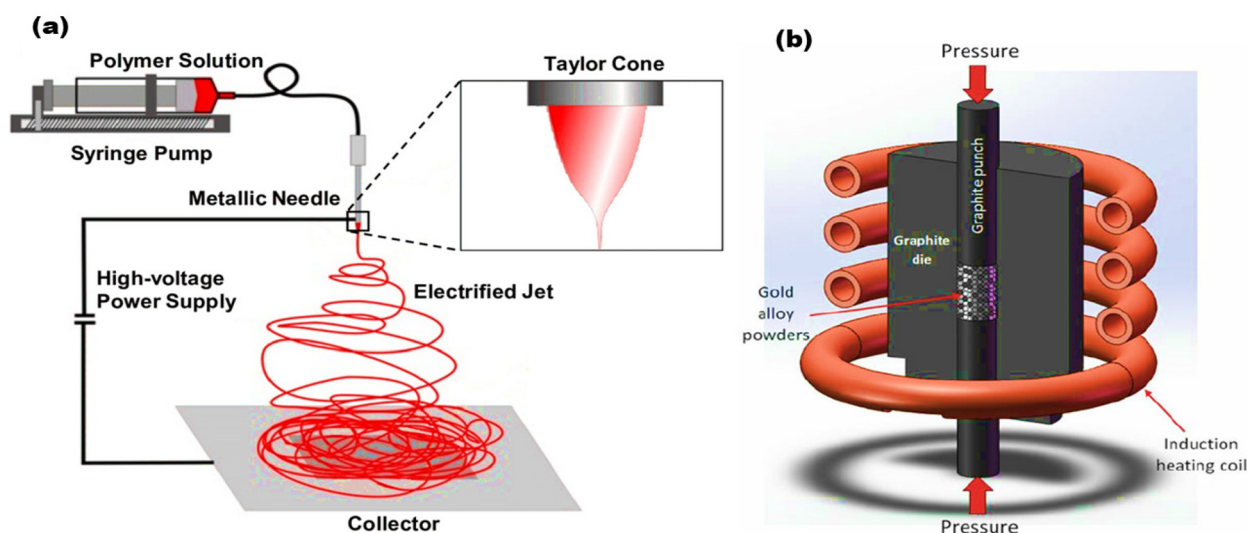


Fig. 4 (a) Electrospinning technology<sup>47</sup> and (b) hot-pressing method.<sup>48</sup>

Fig. 5a illustrates the primary steps of feeding, plasticizing, extrusion, shaping, and chilling. Use of a flat die head with a specially designed retention groove helps guarantee consistent material flow. The automated adjustment device of the die head allows for very precise control over the die lip gap homogeneity. Accuracy can be less than  $\pm 3\%$  for thicker films. Melt extrusion offers more technical benefits, especially for large-scale polypropylene films, when compared to a blow molding thickness control of  $\pm 3\%$ – $5\%$ . Produced either sequentially after melting extrusion or concurrently biaxially oriented, biaxially oriented polypropylene (BOPP) is the most important dielectric polymer for capacitors. In a comparison between the

two approaches, Xiong *et al.*<sup>52</sup> discovered that crystal grains in simultaneously biaxially stretched films are more isotropically distributed than those in sequentially biaxially stretched films. According to Fig. 5b, when the film's thickness is less than  $5\ \mu\text{m}$ , the simultaneous film outperforms the sequential film by at least 10% in terms of the breakdown strength, energy density, and discharge time. To address the issue of filler aggregation and dielectric contrast, Xie *et al.*<sup>53</sup> prepared a range of PP-based nanocomposites using easy high-speed extrusion technology at 900 rpm and a BN/BT hybrid filler. These composites achieved an  $E_b$  of up to  $469\ \text{MV m}^{-1}$  and a high dielectric constant of 2.92. The PP/BT/BN had a signifi-

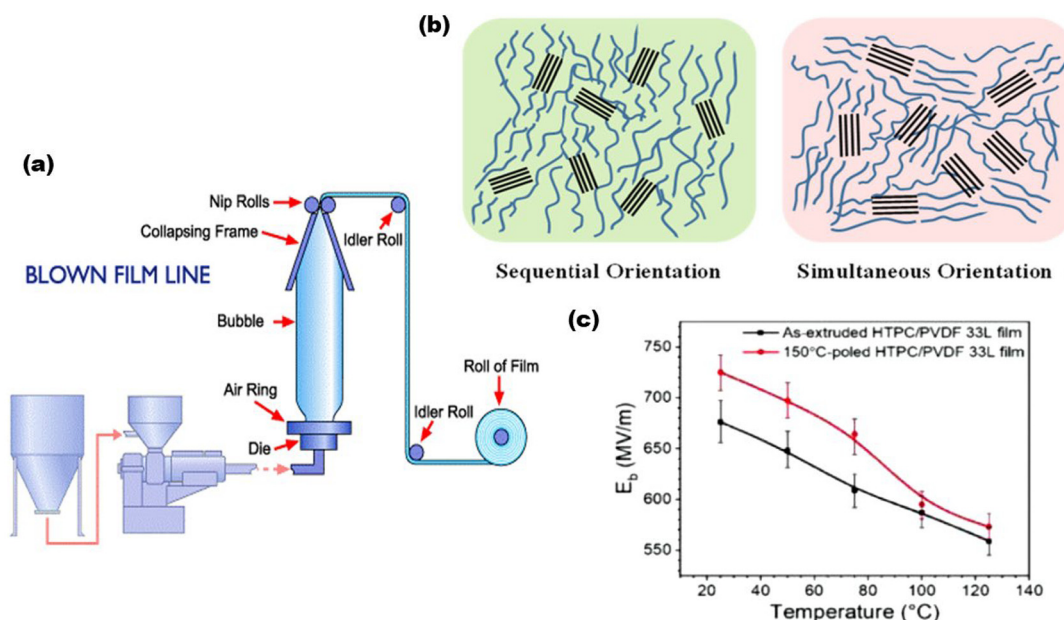


Fig. 5 (a) Extrusion film blowing production line and bubble.<sup>57</sup> (b) Proposed orientation mechanisms of the sequential and simultaneous stretching processes.<sup>58</sup> (c) Breakdown strength of the multilayer film (high-temperature PC/PVDF) with varying number of layers and film thicknesses.<sup>56</sup>



cantly higher energy density than other PP/high-*k* filler composites, measuring 2.82 J cm<sup>-3</sup>. Tan and his colleagues at GE have used melt extrusion techniques to create PEI films. They were able to decrease the film thickness from 10 μm to 3 μm by collaborating with other film manufacturers, including Mitsubishi Plastics Inc.<sup>54</sup> Thinner film extrusion presents additional challenges due to the increased need for improved extrusion process control and faster winding operations. While extruding, using a carrier can help keep creases to a minimum. Collaborating with a film manufacturer from Japan, the GE team enhanced the process of single-layer extrusion of 5, 4, and 3.5 μm PEI films, resulting in wrinkle-free films by controlling winding mechanisms. As an additional demonstration of the free-standing thin films, 3 μm thick letter-size films were manufactured to show that a scale-up melt extrusion of PEI film was feasible. These films do not have wrinkles and have acceptable dielectric properties, with a thickness variation of less than or equal to 5%. In addition, a post-extrusion method was devised that effectively generated a PEI film without wrinkles, which was 3 μm thick and displayed an impressive Weibull breakdown strength of 497.7 kV mm<sup>-1</sup>. A co-extrusion technology was developed by Polymer Plus and Case Western Reserve University (CWRU) to manufacture multilayer polymer films (MLF) with thinner individual layers. These films are suited for thermal plastic resins, such as PP, PVDF, PC, and others.<sup>55</sup> A high dielectric strength resin and a polymer resin with a high dielectric constant were coextruded utilizing an in-house co-extrusion line to create the multi-layered films. A two-layer melt stream is formed when polymers A and B combine in this multi-channel feedback process, as discussed in Fig. 5c. The polymer melt is doubled in thickness by passing it through a succession of multiplier die elements, which slice, spread, and stack the melt to produce a layered structure with anything from a few hundred to several thousand layers. The resins were heated and shaped into a multi-layer structure with thicknesses ranging from 3 to 4097 nanometres, each layer representing an individual layer that is 12 nanometres thick.<sup>56</sup> Two rolls measuring 3000 ft. in length, 12" in width, and 8 μm in thickness were manufactured as part of the manufacturing scale-up for use in metallization and the fabrication of capacitor prototypes. In this investigation, the breakdown strength followed a consistent pattern regardless of the number of layers. There was no discernible difference in the number of layers, but the overall breakdown strength rose as the layer thickness decreased (<200 nm). However, achieving consistency and dependability in scale-up manufacturing could be hindered by the interface quality and extremely thin individual layers.

### 3. Crucial factors for polymer composite dielectrics

Energy storage using polymer composite dielectrics has seen massive development in recent years. However, the majority of these reports were written with room temperature in mind.

Understanding the molecular details of the polymer composite dielectric's microstructure (including ceramic and polymer components), dynamics, dielectric characteristics, and functional mechanism is essential for designing an optimized and innovative polymer nanocomposite dielectric that can operate efficiently at elevated temperatures.<sup>59,60</sup>

#### 3.1 Dielectric permittivity

The dielectric permittivity, often called the dielectric constant, is a measure of a material capacity to retain an electric charge. The dielectric material relative permittivity is the ratio of a capacitor's capability when using that dielectric to that of a comparable capacitor while using a vacuum as its dielectric. The specific  $U_e$  of a film capacitor can be increased by using a dielectric material with high  $\epsilon_r$  values or by reducing the physical magnitude of the capacitor to meet a given energy identification, as stated in eqn (4), in which  $\epsilon$  states that the  $U_e$  of the dielectric material is directly proportional to  $\epsilon_r$ .<sup>61</sup> On the other hand, improving the  $U_e$  performance, particularly at high temperatures, is hindered by lowering  $E_b$ , which happens when  $\epsilon_r$  is large. Calcium copper titanate is said to be an excellent nanofiller because of its large  $\epsilon_r$  and minimal dielectric loss.<sup>62</sup> In both aerospace and HEV applications, concentrated capacitors can help save weight and space. Due to the high replication rate of charge-discharge cycles required by film capacitors with insufficient energy densities, negative side effects including accelerated heating and premature aging might occur.<sup>61,63</sup>

$$U = 0.5\epsilon_0rE^2 \quad (4)$$

#### 3.2 Breakdown strength

The energy density is a quadratic function of the breakdown strength, suggesting that this parameter is the most significant for reaching large energy densities. On the other hand, it is proportional to the dielectric permittivity. However, it is impossible to discount the crucial role of the dielectric permittivity, since it is common for the dielectric permittivity to decrease in conjunction with a rise in breakdown strength. This is because the dielectric permittivity and breakdown strength are inversely related, which is explained by the local electric field concentration that results from the substantial dielectric permittivity differential at the interface of the polymer matrix and fillers. Minimizing the gap between the polymer matrix and filler dielectric permittivity is an encouraging strategy for enhancing the dielectric permittivity without sacrificing the high breakdown strength. Structural engineering methods like surface functionalization, topological design, and interfacial design can make this a reality. The next sections will provide clarification on these structural engineering techniques. The design of dielectric composites with high breakdown strength can be effectively guided by both experimental study and numerical simulations, utilizing the finite element analysis approach.<sup>64</sup> The partial breakdown path that forms in the high electric field area, which can occur when



polymers integrate high quantities of dielectric fillers, was explained by an incomplete breakdown hypothesis. One major problem with using large concentrations of dielectric fillers is that the fillers tend to aggregate. Modifying the current density in polymer composites is greatly influenced by structural designs. The spatial distribution of leakage current density with changeable intensity is clearly depicted *via* the phase field simulation<sup>65</sup> when the proposed structures in polymer composites are tuned (Fig. 6a and b). This provides a roadmap for developing polymer dielectrics with high breakdown strength. The dynamic evolution of the breakdown strength can be predicted by considering the difference in the dielectric strength between nanocomposite-containing nanoparticles and nanofibers. Composites made of polymers and nanoparticles or nanofibers exhibit an evolving breakdown strength (Fig. 6e–g). Nanocomposites made of nanofibers are able to withstand a stronger electric field than those made of nanoparticles.<sup>66</sup>

### 3.3 Dielectric loss

Dielectric loss represents the irreversible conversion of electrical energy into heat within a dielectric material when it is exposed to an alternating electric field. This loss stems from several microscopic processes. One major contributor is dipolar relaxation loss, which occurs when molecular dipoles cannot reorient quickly enough to keep pace with the oscillating field. When the field frequency approaches the intrinsic relaxation time of these dipoles, a phase lag develops between polarization and the applied field, causing significant energy dissipation. Another important component is conduction loss, which arises from the drift of free or trapped charge carriers through the dielectric under high electric fields. Imperfections such as voids, impurities, or weak interfaces in composite dielectrics further amplify these effects by facilitating localized charge accumulation and interfacial polarization. The total dielectric loss is typically represented by the loss tangent ( $\tan \delta$ ), which quantifies the ratio of energy dissipated to energy stored per cycle. High dielectric loss not only reduces

the effective energy-storage density but also leads to Joule heating, thermal instability, and premature electrical breakdown. Therefore, suppressing dielectric loss—through molecular design, purification, nanofiller engineering, and interfacial optimization—is crucial for enabling high-efficiency, high-temperature polymer-based capacitors.

When polarization changes, the stored energy dissipates as charges flow through an electromagnetic field, a phenomenon known as dielectric loss tangent.<sup>67</sup> The capacity to store energy is diminished and an analogous series resistance associated with the capacitor is created when the applied field frequency and relaxation time are similar, a phenomenon known as dielectric loss.<sup>61</sup> Because it contributes to constant heating under high-current circuits, the corresponding series resistance is undesirable. Hence, while making a dielectric capacitor for use at high temperatures, it is crucial to enhance  $\epsilon_r$  while keeping the loss tangent low.

### 3.4 Thermal stability

Thermal stability is an important dielectric feature to take into account while developing a constant dielectric for use in high-temperature applications.<sup>68</sup> How well a material maintains its physical properties when subjected to high temperatures is called its thermal stability. A capacitor ability to store energy depends critically on the dielectric material's thermal stability.<sup>69</sup> A high-temperature dielectric polymer is primarily defined by its glass transition temperature ( $T_g$ ). Amorphous polymers exhibit a quick change in physical characteristics and lose their stiffness when heated over  $T_g$ , according to Li *et al.*<sup>61</sup> As an example, the dielectric characteristics of a polymer material can undergo large fluctuations due to thermal excursion through  $T_g$ , which quickly increases the free volume—that is, the space not occupied by polymer molecules. Furthermore, because of the ease of charge carrier propagation across the material, polymer chains with a high mobility and free volume would provide extensive electrical and ionic conduction. Since these factors affect the stability, dependability, and service life of high-temperature polymer dielectrics,  $T_g$  is

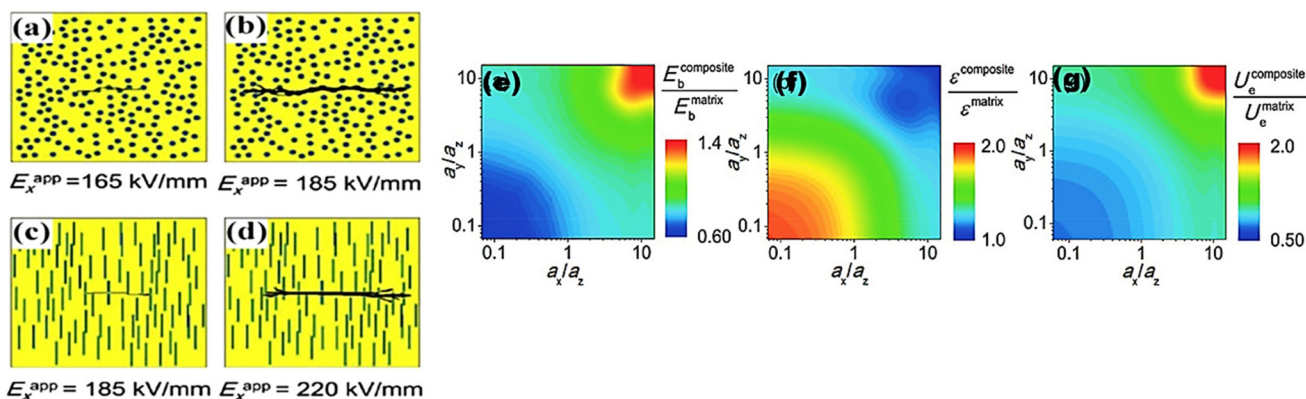


Fig. 6 Breakdown strength evolution process of polymer nanocomposites with the (a) and (b) nanoparticles filler and the (c) and (d) nanofibers at the same volume fraction. (e) The breakdown strength, (f) the effective dielectric permittivity, and (g) the energy density outputted from the high throughput calculation, adapted from ref. 66.



considered the primary metric for evaluating these materials. A dielectric with enhanced dielectric properties, such as a high dielectric permittivity, frequency stability, comparatively low loss tangent, and exceptional dielectric temperature stability under 160 °C, was created by Yang *et al.*<sup>62</sup> using a continuous ultrasonic dispersion technique in conjunction with a solution casting method. The tensile strength of the polymer nanocomposite is more than 60 MPa, and it also has remarkable mechanical characteristics and exceptional flexibility. Using the  $T_m$  to assess the temperature potential is particularly crucial, as are polymers with extremely high crystallinities. The most effective method for achieving high values of  $T_g$  and  $T_m$  is to stiffen the leading chains of polymers by adding hard structural units that prevent rotation.<sup>61</sup> When large side groups are present, it is easy to get high values for  $T_g$  and  $T_m$ . However, these groups physically limit bond rotation, and polar side groups further limit rotation due to polar interactions. By producing intermolecular chemical cross-links that severely limit molecular mobility, a glass transition may not happen, unlike in certain highly cross-linked polymers.

### 3.5 Surface functionalization

Nanoparticles, nanofibers, and nanosheets are just a few of the many filler types used to create polymer nanocomposite dielectrics. The fillers are then functionalized to alter the bond strength and dielectric characteristics at their interface with the matrix. Polymer grafting to create a non-smooth layer (such as a star-shaped polymer as a nanoreactor) is one of several methods that have been documented. Another is polymer coating. Here, we will mostly discuss traditional ceramic fillers like SrTiO<sub>3</sub>, as well as their doped forms, which have a reasonably high dielectric permittivity. For better filler dispersion and interfacial compatibility with the polymer matrix, a variety of surface modifiers were employed, as shown in Table 2. We can find PVDF and P(VDF-HFP) among the polymer matrix materials listed in the table. Researchers have looked at both organic and inorganic substances that can modify surfaces. Table 2 also summarizes the enhanced dielectric permittivity, dielectric loss, breakdown strength, and energy density attributes. The breakdown strength and desired dielectric properties of nanocomposite dielectrics can be fine-tuned by adjusting the ceramic filler amount and surface modifiers. Achieving high dielectric permittivity or breakdown strength can be aided by surface functionalization, which does double duty by enhancing interfacial compatibility and reducing filler agglomeration in polymer matrices. For example, a highly conductive network was produced by employing PVA as barriers to manufacture RGO/PVA porous composites, which led to an efficient and innovative process of unidirectional freeze drying.<sup>70</sup> This technology was discovered to boost the high dielectric permittivity and lower the loss tangent by using the PVA as a barrier between the aligned conductive networks. In addition, microlaminated composites with conductive RGO-PU layers were isolated by BN-PU, leading to a low dielectric loss of 0.091 and a high dielectric permittivity of 1084.<sup>91</sup>

### 3.6 Other parameters that affect polymer composite dielectrics

Composite dielectric performance is highly dependent on the filler particle shape. As an example, research into the effect of the particle shape and size on the dielectric tunability of nanocomposites has shown that larger plate-like (Ba<sub>0.6</sub>Sr<sub>0.4</sub>)TiO<sub>3</sub> nanoparticles in PVDF-textured composites have a better dielectric property.<sup>56</sup> The two-step molten salt process allows for controlling soaking time to alter the particle size to that of a plate. Also, a form factor in the dielectric theoretical model allows for characterisation of the particle size using composite dielectric property simulations, which is in good agreement with the experimental findings. As a result, (Ba<sub>0.6</sub>Sr<sub>0.4</sub>)TiO<sub>3</sub>/PVDF nanocomposites reach their ideal dielectric at a specific nanoparticle size. In order to decrease the aggregation and the likelihood of forming conductive paths in composites, new types of structured fillers such as core-shell-like,<sup>56,57</sup> surface functionalized two-dimensional,<sup>58</sup> and hollow-structured<sup>59</sup> fillers are being used. These fillers form multiple interfaces in hierarchical or gradient-layered structures<sup>60</sup> and help to suppress the dielectric loss of composites.<sup>61</sup> Based on experimental and simulation results, it was found that polymer nanocomposites with BST nanowires had improved electrical displacement and reduced inhomogeneity of the electric field distribution, in contrast to other fillers such as BST nanorods, pure polymers, and BST nanoparticles.<sup>62</sup> This finding lends credence to the idea that the shape of the ceramic filler has an impact on the breakdown strength and dielectric property of the composites. Composites containing BST nanowires exhibit improved energy density, which is because BST nanowires have a high aspect ratio.

Among the key parameters influencing the dielectric properties of polymer composite dielectrics, the shape and size of the incorporated fillers play a critical role. The filler size directly affects the interfacial area and polarization behavior. Nanoscale fillers create a much larger interfacial region with the polymer matrix, enhancing interfacial polarization and improving dielectric permittivity, while also reducing the risk of local electric-field concentration that can trigger premature breakdown. Conversely, larger micro-sized fillers often lead to poor dispersion and increased defect density, resulting in higher dielectric loss and weakened breakdown strength. The filler shape further determines the effectiveness of charge transport suppression and field distribution within the composite. High-aspect-ratio structures—such as nanowires, nanosheets, or nanotubes—establish percolative pathways at lower filler loadings, boosting permittivity but sometimes increasing leakage risk if not properly insulated. Spherical or near-spherical nanoparticles, on the other hand, tend to disperse more uniformly and maintain low dielectric loss but contribute less strongly to permittivity enhancement. Thus, tailoring the filler geometry and dimension is essential for optimizing the delicate balance between high permittivity, low loss, and strong breakdown performance in dielectric polymers.





**Table 2** Summary of the dielectric, breakdown strength, and energy density characteristics of the various surfactants and fillers that are utilized in dielectric composites

S. no.	Author	Polymer matrix	Dielectric filler content	Surface modifier	Dielectric permittivity (1 kHz)	Dielectric loss (1 kHz)	Breakdown strength (kV mm <sup>-1</sup> )	Energy density (J cm <sup>-3</sup> )	Ref.
1	D. P. Kim, J. P. Tillotson <i>etc.</i>	P(VDF-HFP)	50 vol% BaTiO <sub>3</sub> particles	Phosphonic acid	31	0.03	215	3.2	71
2	Y. Niu, F. Xiang, <i>etc.</i>	PVDF	50 wt% BaTiO <sub>3</sub> particles	Carboxylic acid	32	0.04	325	9.89	72
3	Z.-H. Dai, T. Li, Y. Gao <i>etc.</i>	Poly(vinyl alcohol)	40 vol% BaTiO <sub>3</sub> particles	Galic acid	51	0.08	144	0.554	73
4	J. Fu, Y. Hou, <i>etc.</i>	PVDF	40 vol% BaTiO <sub>3</sub> particles	Polyvinyl pyrrolidone (PVP)	65	0.02	10	0.03	74
5	K. Yu, H. Wang <i>etc.</i>	PVDF	20 vol% BaTiO <sub>3</sub> particles	NXT-105	41	0.03	200	3.54	75
6	K. Yu, Y. Niu <i>etc.</i>	PVDF	10 vol% BaTiO <sub>3</sub> particles	Tetrafluoro phthalic acid	35	0.04	285	5.1	76
7	H. Luo, D. Zhang <i>etc.</i>	P(VDF-HFP)	20 vol% BaTiO <sub>3</sub> particles	Hydantoin resin	20	0.04	330	8.13	77
8	P. Hu, S. Gao <i>etc.</i>	PVDF	4 vol% BaTiO <sub>3</sub> particles	Titanate coupling agent	12	0.04	517	11.27	78
9	K. Yu, Y. Niu <i>etc.</i>	PVDF	10 vol% BaTiO <sub>3</sub> particles	Polyvinylpyrrolidone (PVP)	14	0.02	336	6.8	79
10	S. Liu, J. Zhai, <i>etc.</i>	PVDF	2.5 vol% SrTiO <sub>3</sub>	Polyvinylpyrrolidone (PVP)	11	0.04	380	6.8	80
11	G. Wang, X. Huang <i>etc.</i>	P(VDF-HFP)	Nanofibers 5 vol% BaTiO <sub>3</sub> nanowires	Fluoro-polydopamine	14	0.04	480	12.87	81
12	H. Tang, H. A. Sodano <i>etc.</i>	PVDF	7.5 vol% Ba <sub>0.2</sub> Sr <sub>0.8</sub> TiO <sub>3</sub>	Ethylenediamine	17.5	0.09	484.3	14.86	82
13	H. Tang, Y. Lin	P(VDF-TrFE)	17.5 vol% BaTiO <sub>3</sub> nanowires	Ethylenediamine	69	0.09	300	10.48	83
14	H. Luo, Z. Wu <i>etc.</i>	CFE-P (VDF-HFP)	15 vol% BaTiO <sub>3</sub> platelets	Polydopamine H <sub>2</sub> O <sub>2</sub> and DN-101	20	0.03	175	9.01	84
15	L. Gao, J. He	PVDF	10 vol% BaTiO <sub>3</sub> particles	Polydopamine H <sub>2</sub> O <sub>2</sub> and DN-101	20	0.05	260	9.01	85
16	H.-J. Ye, W.-Z. Shao	PVDF	40 vol% BaTiO <sub>3</sub> nanoparticles	1-Tetradecylphosphonic acid	48	0.03	250	7	86
17	Y. Kim, O. N. L. Smith	P(VDF-HFP)	50 vol% BaTiO <sub>3</sub> particles	PFBPA	30	0.03	250	7	87
18	K. Yang, X. Huang	P(VDF-HFP)	50 vol% BaTiO <sub>3</sub> particles	PHFDA	45	0.02	182.6	6.23	88
19	S. Liu, S. Xue	PVDF	7.5 vol% BaTiO <sub>3</sub> nanowires	3-Aminopropyltriethoxysilane	24	0.018	230	5.6	89
20	P. Hu, Y. Song	P(VDF-TrFE)	4.1 vol% Bi <sub>2</sub> O <sub>3</sub> -doped Ba <sub>0.3</sub> Sr <sub>0.7</sub> TiO <sub>3</sub> fibers	<b>Polydopamine</b>	<b>16</b>	<b>0.02</b>	<b>227.5</b>	<b>4.72</b>	<b>90</b>

### 3.7 Failure mechanism of dielectric polymers

Dielectric polymers are known for exhibiting a graceful failure mechanism, a phenomenon where the material undergoes progressive and controlled degradation, rather than abrupt electrical breakdown. When subjected to high electric fields, thermal fluctuations, or mechanical loading, the polymer matrix absorbs and redistributes localized stresses through its inherent chain mobility and viscoelastic nature. This ability allows polymer chains to undergo rearrangement, segmental motion, and local relaxation, which helps dissipate the accumulated energy and prevents sudden catastrophic failure. Microscopically, defects such as voids, molecular imperfections, or impurities often act as initial sites for charge injection or partial discharge. Instead of allowing these defects to trigger instantaneous breakdown, dielectric polymers mitigate the impact through polarization relaxation, field redistribution, and space-charge trapping. As electric trees or micro-cracks begin to form, they typically propagate slowly due to the polymer's flexibility and capacity to resist crack acceleration. The gradual growth of these damage structures leads to a slow increase in the leakage current and a stepwise reduction in the dielectric strength, rather than an immediate collapse. Thermal effects also contribute to graceful failure. As the polymer heats locally under an electric field, it can soften slightly, enabling further field relaxation, defect healing, or redistribution of charges. Additionally, the presence of deep traps—common in polymer nanocomposites—helps delay full breakdown by capturing high-energy electrons and preventing avalanche conduction.

This progressive failure pathway has significant advantages: it improves safety, enhances operational reliability, and allows early detection through measurable changes such as increased dielectric loss, partial discharge activity, or rising leakage current. Due to this predictable and non-catastrophic failure behavior, dielectric polymers are widely used in capacitors, insulation systems, flexible electronics, and emerging high-temperature energy-storage materials, where durability and fail-safe performance are essential. A comprehensive and universally accepted theory that explains the direct relationship between the chemical composition of dielectric polymers and their self-clearing behavior has not yet been established. Existing studies suggest that polymers with a high ratio of carbon to (hydrogen + oxygen) generally exhibit poor self-clearing performance. This is because, during electrical breakdown, excessive carbon can be liberated and subsequently form conductive carbonaceous channels that inhibit the isolation of the defect site and prevent full recovery of the insulating properties.<sup>92</sup> In contrast, polymers with a lower carbon-to-(hydrogen + oxygen) ratio tend to demonstrate more effective self-clearing, as the reduced carbon content limits the formation of conductive residues and promotes the development of localized non-conductive voids after breakdown. Fig. 7 compares the ratio of (carbon + nitrogen + sulfur) to (hydrogen + oxygen) for the dielectric polymers under discussion, highlighting compositional variations that may influence their clearing

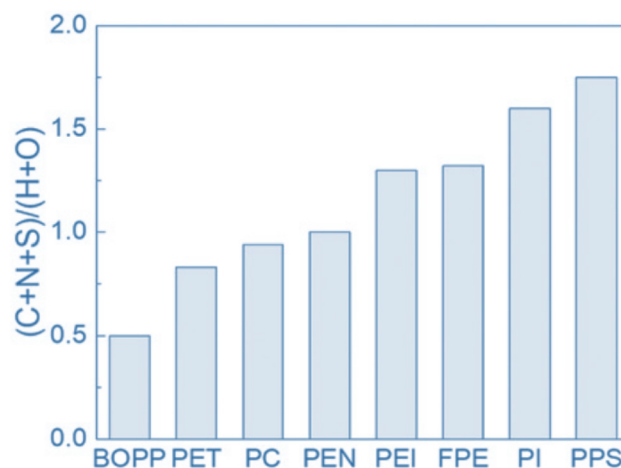


Fig. 7 The ratio of (carbon + nitrogen + sulfur) to (hydrogen + oxygen) of high-temperature dielectric polymers.

behaviour. Furthermore, polymers containing additional elements—such as fluorine, chlorine, or other heteroatoms—not included in the typical CHONS composition set require deeper evaluation, as these elements may modify decomposition pathways, influence by-product formation, and potentially alter the self-clearing efficiency. Continued investigation into these compositional effects is essential for establishing clearer design rules for next-generation self-healing dielectric materials.

## 4. Low dielectric loss media for high-power energy transmission

Low dielectric loss media are crucial for high-power energy transmission applications, especially in high-voltage capacitors and transmission systems, because they minimize energy dissipation as heat and thus improve efficiency, reliability, and thermal stability. Recent advances have produced several promising polymer systems and nanocomposites that combine ultra-low dielectric loss with other desirable properties. For instance, Zhao, Sun, and Fang (2024) synthesized high-temperature polymers containing bulky adamantane linkers and benzocyclobutene units, achieving a remarkably low dielectric loss ( $Df \approx 1.94 \times 10^{-3}$ ) at 10 GHz while maintaining excellent thermal stability (glass transition temperature  $>350$  °C).<sup>93</sup>

Jiaren Hou, Jing Sun, and Qiang Fang<sup>94</sup> also reported on oxygen-free polymers with extremely low loss ( $Df \sim 6.4 \times 10^{-4}$ ), highlighting how careful molecular design (removing oxygen atoms and introducing  $-CF_3$  groups) can suppress polarization losses. By the perspective of capacitive energy storage, a recent comprehensive review highlighted dilute nanocomposites—polymer matrices with very low filler loading—as a powerful strategy: by using ultralow concentrations of nanoscale inorganic particles, one can boost permittivity while maintaining high breakdown strength and very low dielectric loss.<sup>95</sup> In the context of power transmission, especially when dealing with



high voltages and high fields, dielectric polymers also need to manage not just electrical loss but thermal management. A breakthrough reported in *National Science Review* showed a ladderphane copolymer with a very high intrinsic thermal conductivity ( $\sim 1.96 \text{ W m}^{-1} \text{ K}^{-1}$ ) and very low electrical conductivity, enabling capacitive performance at elevated temperatures with reduced conduction and heating losses.<sup>96</sup> Moreover, research in polyolefin/graphene nanocomposites is advancing rapidly: a 2024 review highlighted progress in polyolefin (e.g., polypropylene) matrices filled with graphene to achieve a high dielectric constant and low dielectric loss, which could be particularly useful for lightweight, high-voltage insulation applications.<sup>97</sup> Finally, another promising direction is in high-performance low-loss polybenzoxazine-based composites, which combine thermal stability with low dielectric loss, making them potentially useful for high-frequency and high-power transmission systems.<sup>98</sup>

Energy storage for high-current transmission across power grids is the main application of dielectric capacitors. Minimizing the dielectric loss of polymer-based dielectrics is crucial for mitigating the heating effect caused by power equipment and high current. Even though the BOPP dielectric constant is quite small at 1 kHz (2.2), its dielectric loss is incredibly low at 1 kHz ( $< 0.0002$ ). As a result, it is one of the most widely used dielectric capacitors as the primary energy storage medium in electrical grids to this day,<sup>99</sup> and it produces very little heat as a result of dielectric loss.<sup>100</sup> The dielectric loss of PVDF and PVDF-based materials is substantially higher than that of BOPP ( $> 0.02$ ),<sup>101</sup> severely limiting the materials' potential uses. In ferroelectric polymers, dielectric loss primarily arises from two mechanisms: ferroelectric loss and conduction loss. Ferroelectric loss occurs when the applied alternating electric field fails to remain synchronized with the switching of ferroelectric dipoles, leading to energy dissipation during repeated polarization–depolarization cycles. Conduction loss, on the other hand, results from leakage current generated by the migration of charge carriers through the polymer under high electric fields. Together, these loss mechanisms can significantly degrade the dielectric performance and energy-storage efficiency of ferroelectric polymer-based capacitors.<sup>102</sup> By preventing leakage current, researchers have discovered that multilayered nanocomposites can decrease dielectric loss by suppressing conduction losses. A multilayered nanocomposite made of P(VDF-HFP)/P(VDF-TrFE-CFE) achieved an unprecedentedly high charge discharge efficiency of 80% to 85% when it was created by Jiang *et al.*<sup>103</sup> A decrease in production costs and an expansion of industrial applications can be achieved by modifying the molecular structure of polymer-based materials to decrease dielectric loss. The team led by Chen achieved a very high discharge efficiency of 90% and a low dielectric loss of less than 0.006 by constructing an asymmetrical alicyclic amine-polyether amine molecular chain structure inside a crosslinked epoxy network.<sup>104</sup> To further decrease ferroelectric loss in the PSF/PVDF system, PVDF crystallization confinement is another technique. In theory, the ions' mobility is limited by the “barrier effect” provided by the

well-oriented crystals. In addition, free radical polymerization of polystyrene (PS) onto P(VDF-CTFE) results in significantly decreased dielectric loss compared to PVDF. The dielectric loss is reduced after PVDF crystallization because PS forms a restricted layer around the PVDF crystal, as opposed to when pure PVDF is added. The best attributes are attained at a 30% PS grafting ratio, with a reasonably high discharge energy density ( $10 \text{ J cm}^{-3}$  at  $600 \text{ MV m}^{-1}$ ) and a low dielectric loss (0.006 at 1 kHz).<sup>105</sup> Reducing compensatory polarization in the polymer can be achieved by promoting quick dipole reorientation during discharge and limiting the ferroelectric domains.<sup>106</sup>

#### 4.1 High-temperature dielectric polymer engineering

A high-temperature, ultra-pure PP resin was developed a decade ago by engineers and scientists. Japanese and European film manufacturers (Toray Industries) have recently developed a high-temperature polypropylene that can withstand temperatures of 125 °C or higher. The performance of capacitors for high-temperature energy storage and conversion is limited by important considerations, such as the reduced breakdown strength, increased deformation, and dielectric loss at increasing temperatures. The film leakage current spikes when subjected to thermal and electrical field stimulation, leading to significant energy loss, and poor capacitance performance and charge–discharge efficiency. Several dielectric breakdown mechanisms (thermal runaway, free volume breakdown, and electromechanical breakdown) become more or less involved in the dielectric breakdown issue in the absence of high-temperature dielectric polymers. Because of their poor thermal conductivity, polymers can quickly experience electrical breakdown in the event of thermal runaway. When electron acceleration begins and the polymer chains are attacked, the free volume within the polymer also plays an active role in the breakdown process.<sup>107</sup> Polymers can undergo what is known as electromechanical breakdown when subjected to a strong electric field, which causes a reduction in their elastic modulus and thickness as a result of the Maxwell electrostatic stress.<sup>108</sup> To circumvent these thermal-mechanical degradations, it is preferable to use polymer films that are both rigid and heated to high temperatures. Improved breakdown strength and minimal dimensional change at increased temperatures are two encouraging properties of inorganic coatings.<sup>109</sup> Polymer-based dielectric materials hold significant promise as energy-storage media for electrostatic capacitors. However, their inherently limited thermal resistance causes severe degradation in dielectric energy-storage performance at elevated temperatures, restricting their utility in harsh environments. J. Wang *et al.*<sup>110</sup> introduced a flexible laminated polymer nanocomposite, in which the polymer phase is confined at the nanoscale, resulting in enhanced thermal, mechanical, and electrical stability. The nanolaminate structure—comprising a nanoconfined polyetherimide (PEI) sandwiched between solid  $\text{Al}_2\text{O}_3$  layers—achieves an impressive energy density of  $18.9 \text{ J cm}^{-3}$  and an energy efficiency of  $\sim 91\%$  at 200 °C. Nanoconfinement of the PEI polymer reduces its



diffusion coefficient and restricts thermal molecular motion, yielding a remarkable 37 °C increase in the glass-transition temperature when compared to bulk PEI. The synergistic effects of nanoscale confinement and interfacial charge trapping within the laminated structure significantly enhance the electrical breakdown strength and energy-storage performance over a wide temperature range up to 250 °C. Furthermore, by applying the flexible ultrathin nanolaminate onto curved surfaces such as thin metal wires, we demonstrate a novel approach for constructing highly efficient, compact metal-wired capacitors capable of achieving substantial capacitance despite their minimal device volume. Several published studies show that crosslinking is an effective technique to limit the motion of molecular chains. These studies also show that film capacitors are more efficient, have less dielectric relaxation, and have better breakdown strength. The dielectrics currently used for high working temperature film capacitors can be selected from polymers with high glass transition temperature  $T_g$ , such as polyimide (PI), poly(etherimide) (PEI), fluorene polyesters (FPEs), poly(ether ether ketone) (PEEK).<sup>19</sup> Their physical properties are detailed in Table 3.<sup>103</sup> One example is a nanocomposite that significantly reduces conduction loss at high temperatures and achieves a high breakdown field. These nanocomposites are made of cross-linked high-temperature glass transition polymer (BCB) and 10% boron nitride nanosheets (BNNS).<sup>111</sup> No other commercially available high temperature polymer can match the 90% charge/discharge efficiency ( $\eta$ ) that c-BCB/BNNS displays at 150 °C up to 400 MV m<sup>-1</sup>, as demonstrated in Fig. 8a and b. While most

other commercial polymers do not exhibit any significant charge storage performance at temperatures as high as 250 °C (Fig. 8c and d) and 200 °C, c-BCB/BNNS retains a breakdown strength of 400 MV m<sup>-1</sup> with a comparatively high  $\eta$ . One type of amorphous polar glass-phase dielectric polymer is aromatic polythiourea (ArPTU). It can be made by combining 4,4'-diphenylmethane diamine (MDA) and thiourea in *N*-methyl-2-pyrrolidone (NMP) using microwave-assisted polycondensation with *p*-toluene sulfonic acid as a catalyst. The resulting powder can be white or yellowish, and it can then be dissolved in *N,N*-dimethylacetamide. The solution cast ArPTU film has a maximum electrical energy density of more than 24 J cm<sup>-3</sup>, a dielectric breakdown strength of more than 1.1 GV m<sup>-1</sup>, and a low loss at high electric fields of 10% at 1.1 GV m<sup>-1</sup>.<sup>112</sup> For high voltage energy storage, ArPTU films with a thickness of 5–10  $\mu$ m outperform other high-temperature dielectrics such as aromatic polyurea, polycarbonate, polyester, and polyimide. Singh, M., *et al.*<sup>113</sup> reported on a polymer thin film heterostructure-based capacitor of poly(vinylidene fluoride)/poly(methyl methacrylate) with stratified 2D nanofillers (mica or h-BN nanosheets) (PVDF/PMMA-2D fillers/PVDF), that shows enhanced permittivity, high dielectric strength and an ultra-high energy density of 75 J cm<sup>-3</sup> with efficiency over 79%. Ding, J., *et al.*<sup>114</sup> demonstrated that high-temperature polymer dielectrics with high energy density are urgently needed for advanced capacitive energy-storage applications. However, severe conduction losses at elevated temperatures lead to a sharp decline in the capacitive performance of polymers, limiting their practical deployment. In this work, high-electron-affinity polymer dots (PDs) were incorporated into high-temperature polymers to fabricate all-organic nanocomposite dielectrics *via* solution casting. These PDs efficiently capture injected electrons through strong electrostatic interactions, thereby suppressing charge transport and accumulation within the composites. As a result, the leakage current density is substantially reduced and the high-temperature energy-storage capability is significantly enhanced. The nanocomposites show more than a 2.5-fold improvement in high-temperature capacitance compared to pristine polymers. For instance, the PEI/PD system achieves an energy density of 3.24 J cm<sup>-3</sup>, along with

**Table 3** Physical properties of polymers with high temperature stability<sup>118,119</sup>

Polymer	$\epsilon$	The highest working temperature/°C	$\tan \delta$	Discharge efficiency
PC	3.2	125	0.0013	~90%
PEEK	3.2	150	0.004	~90%
FPE	3.5	200	0.0025	—
PEI	3.2	200	0.01	~96%
PI	3.1	150	~0.017	~94%

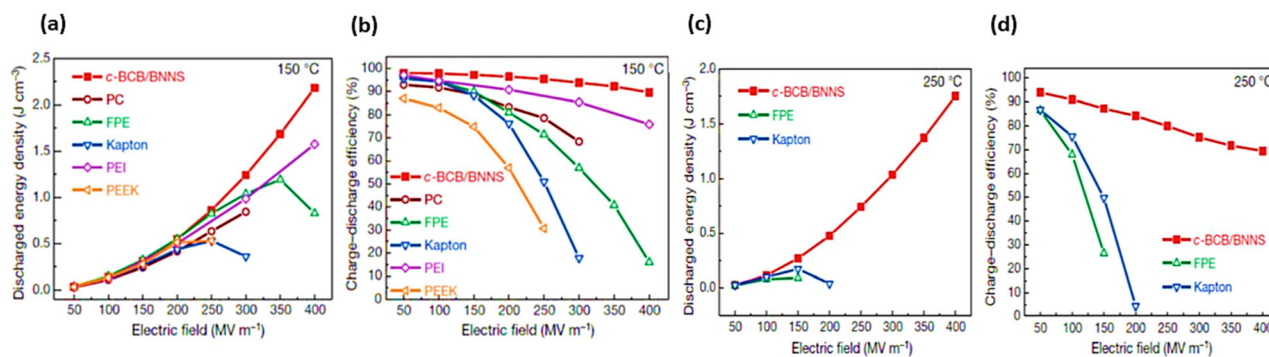


**Fig. 8** (a and b) Electrical energy storage capability. Discharged energy density and charge–discharge efficiency of c-BCB/BNNS with 10 vol% of BNNSs and high- $T_g$  polymer dielectrics measured at 150 °C and (c and d) 250 °C, adapted from ref. 111.



excellent electrical fatigue resistance over 20 000 cycles.<sup>115,116</sup> The study offers a simple and universal strategy to address the challenge of low discharged energy density in polymer dielectrics operating under high-temperature conditions.

In the development process of thin polymer films, a common practice of increasing the mechanical and dielectric strength of polymer films is the biaxial orientation or stretching method. It often works well with melt extrusion for many polymers like PP, PEN, PET, nylon, PC, and PVDF-HFP to meet the requirements of both decreased thickness and increased dielectric strength. With the increasing need and investigation for high-temperature dielectric polymers, this method has also been applied to high-temperature polymers like PTFE, PEI, and PPS. For instance, the W. L. Gore company has successfully developed a manufacturing process for dense PTFE films capable of servicing at >200 °C, combining the rapid stretching and controlled sintering process.<sup>117</sup> They started with a porous or thick solid PTFE film heated up to a softening temperature, then stretching the porous film during a densification process to achieve a thickness reduction under suitable stress in MD and/or TD. W. L. Gore has patented this process for its expanded PTFE film and successfully converted the porous PTFE film in the range of 3–10 μm into dense PTFE films. As a high-temperature polymer (>250 °C), the PTFE films exhibit very high dielectric strength (>650 kV mm<sup>-1</sup>), extremely low dielectric loss (<0.0005), high mechanical strength (>10 MPa), and good adhesion with an aluminium electrode with self-clearing capability. The concern for the PTFE film and its capacitor products is the high film surface roughness and severe self-clearing events at service temperature and voltage.

#### 4.2 Frequency response for energy storage dielectrics

There are several industries in which the response time is crucial, such as pulsed power equipment. Pulsed power systems transfer all of their stored energy to the load in a fraction of a second.<sup>120</sup> In Fig. 9, we can see the standard layout of a Marx pulse bank. New weaponry, including inertial restraint systems, laser guns, and high-power microwaves, rely on power pulse devices that operate on a timescale of 1 nanosecond or less. In this case, high-energy storage density is not necessary; the energy storage medium just needs to be able to react very

rapidly. The energy discharge frequency needs to be 1 GHz to produce a pulse with a millisecond front edge. However, this threshold is unattainable for most polymers due to their main chains and pendant dipole structures.<sup>121</sup> Thus, to solve this “frequency problem”, a specialized molecular design has to be carried out. Research by Stephanovich *et al.*<sup>122</sup> indicates that PVDF and its copolymers allow for a gradual discharge process, leading to a reduction in energy released in the power pulse system. Results showed that BOPP and P(VDF-CTFE)-g-PS discharged more quickly than PVDF, according to Guan *et al.*,<sup>106</sup> who established the experimental time  $t_0$  as the amount of time it took for the load's discharged energy to reach 90% of the final value. The reason behind this is that the linear dielectric materials used in BOPP do not promote the formation of space charge. Less space charge is induced in the sample with P(VDF-CTFE)-g-PS because of the confinement effect caused by the nonpolar PS interfaces surrounding the PVDF crystals. By combining the reversible nonpolar and polar molecular structures, Chu *et al.*<sup>123</sup> demonstrated that defect-modified PVEF polymers can achieve a high energy density (>17 J cm<sup>-3</sup>), a fast discharge speed (<1 ms), and low dielectric loss. This achieves high  $D$  with the proper dielectric constant, preventing early D-saturation. However, the field basic mechanisms and associated structure–property connections have not yet been thoroughly investigated.

#### 4.3 Limitations of polymer dielectrics in high-temperature applications

When working at high temperatures, there are two primary challenges to using dielectrics made of polymers. One issue is that dielectric polymers typically have a low glass transition temperature ( $T_g$ ), which makes their thermal stability weak.<sup>125</sup> Polymers undergo a dramatic change in their dielectric property compared to ambient temperature when heated beyond  $T_g$ , becoming pliable and displaying strong chain segment movements. Take polymer chains as an example, their high mobility makes them ideal for charge carrier movement, which in turn increases conduction loss and the likelihood of dielectric materials failing. Zhu *et al.* created multi-layered all-polymer dielectric films with good high-temperature capability and high dielectric permittivity.<sup>126</sup> Polymers have poor

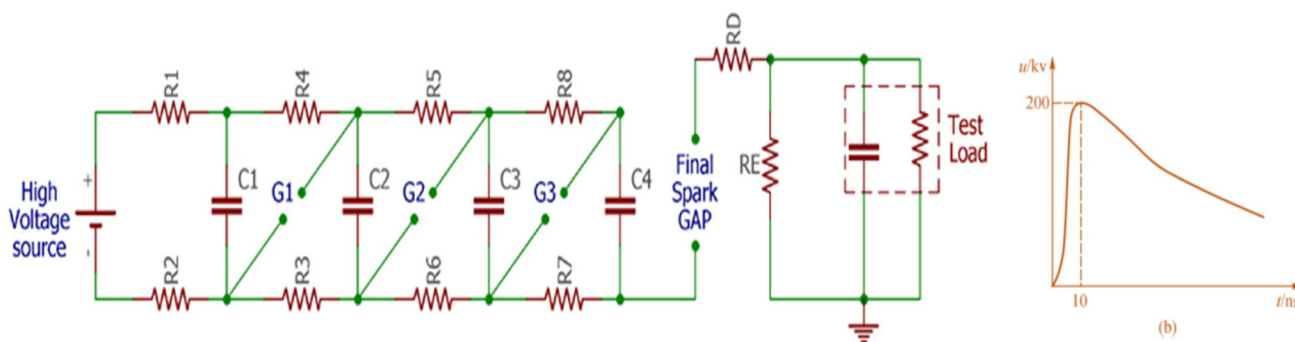
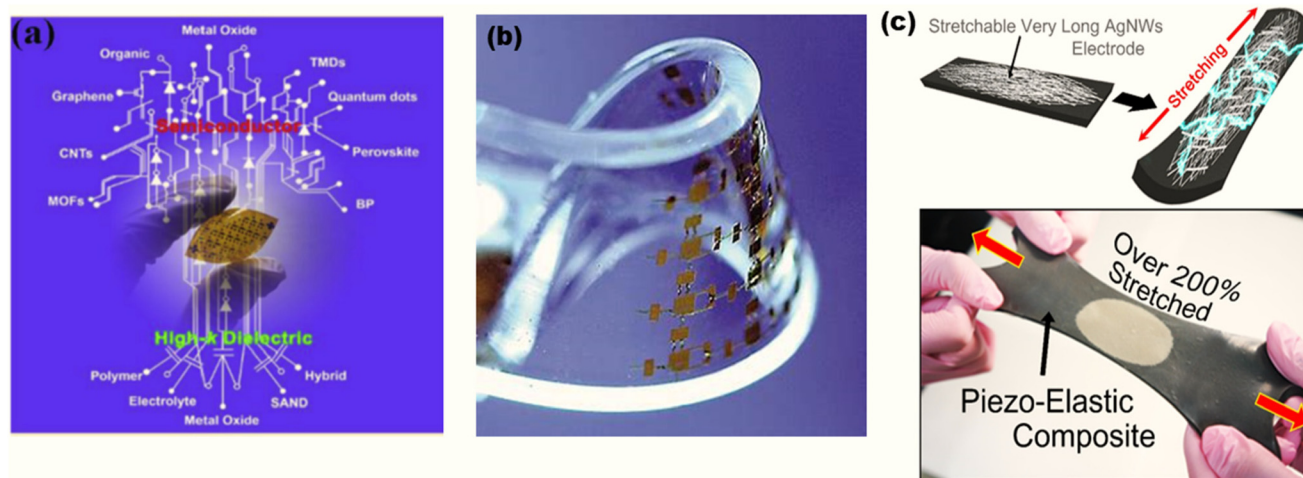


Fig. 9 Schematic of the Marx pulse bank and nanosecond pulse waveform.<sup>124</sup>





**Fig. 10** Recent advances in the flexible polymer composite dielectrics: (a) gate dielectrics for flexible electronics reproduced from ref. 13 with permission from ACS, copyright 2018. (b) Stretchable organic electronics by integrating an elastomer matrix and organic semiconducting polymer adapted from ref. 137 (credit <https://www.azom.com>). (c) Electronics of the hyper-stretchable elastic composite dielectrics.<sup>138</sup>

thermal stability because of their weak inter- and intra-molecular interactions. For example, a film made of nonaromatic polyarylene ether nitrile resin had stable dielectric permittivity and loss up to 300 °C.<sup>127</sup> Conversely, dielectrics made of polymers typically have a high leakage current when subjected to high temperatures. This is because nearly all of the conduction mechanisms in polymers—including bulk limited and electrode limited conduction events like Schottky emission, thermionic-field emission, Poole-Frenkel emission, hopping conduction, and ohmic conduction—are positively scaled with temperature. Encouraging stronger chemical bonds like hydrogen bonds (*e.g.*, –NH–, –CO–NH–),  $\pi$ -conjugation in polymer chains (*e.g.*, imide ring, imidazole ring), aromatic/heteroaromatic molecular skeletons, and high-strength chemical bonds (*e.g.*, C–F) is a common approach to enhance the thermal stability of polymers. Because of their well-established processing methods and comparatively high thermal stability, the high-temperature polymers are good candidates for use in the development of capacitor dielectrics. There are a number of recently created compounds that show promise as high-temperature polymer dielectrics, in addition to these commercial polymer films. Some examples of such work include a fluorene polyester (FPE)<sup>128</sup> modified chemically by Venkat *et al.* that exhibits excellent dielectric stability with increasing temperature, and a thin film of high-temperature poly(phthalazine ether ketone) that can provide an energy density of 2 J cm<sup>-3</sup> at 190 °C, synthesised by Pan *et al.*<sup>129</sup> Polymer dielectrics dissipate more Joule heat when their electrical conductivity increases with temperature. This is because an increase in the material internal temperature causes the electrical conductivity to rise. The so-called thermal runaway would happen when the positive feedback mentioned earlier arises, leading to thermal breakdown.<sup>130</sup> Because of the thermal runaway phenomena, high-temperature polymers with a high  $T_g$  do not guarantee continued functioning in environments with

high electric fields and temperatures. Reducing the conduction loss and increasing the thermal conductivity in polymer-based dielectrics are two good ways to deal with this issue.

## 5. Recent progress in flexible and stretchable polymer composite dielectrics

The remarkable flexibility and high dielectric strength of flexible and stretchy polymer composite dielectrics have recently garnered a great deal of interest.<sup>131</sup> High breakdown strength, superb dielectric permittivity, outstanding energy density, and promising mechanical properties are some of the desirable properties of flexible polymer composite dielectrics that are being proposed to fulfil the growing demands of electronics. For the purpose of achieving extraordinary electroelastic characteristics, hyperelastic materials with a high dielectric permittivity are filled with liquid-metal microdroplets, rather than having the stiff fillers integrated into the polymer matrix.<sup>132</sup> The fabrication of high-performance flexible organic field-effect transistors based on polymer-ceramic dielectric composites has enormous potential in building portable organic electronics. These transistors are made by integrating dielectric polymer with new ceramic particles. Binary polymer composite dielectrics, including PVDF-HFP/PVP or polyacrylic acid/poly (methyl methacrylate) acid, are also used to create low-voltage-driven field-effect transistors, which are flexible electronic devices that can be controlled in response to both deformation and low voltage stimuli.<sup>133,134</sup> The versatility of flexible electronics has been enhanced by recent developments in polymer composite dielectrics. For example, thin film transistors that exhibit the ideal combination of mechanical deformation and dielectric property can be created using dielectric



gates made of high-dielectric permittivity dielectrics (Fig. 10a), and a combination of material concept design and fabrication techniques. We still need to find dielectric materials with the right dielectric permittivity to make flexible electronics that are safer for the environment and work better. The development of low-field-emission flexible optoelectronics with transparent, mechanically stretchy, and self-healing dielectrics is being pursued in order to advance electronic skins for wearable electronics and soft robots.<sup>135</sup> Additionally, optoelectronic dielectrics exhibit excellent elasticity, allowing for stretching of up to 20%. Fabricating low-voltage synaptic transistor arrays using the inkjet printing technology allows for the smooth interaction of flexible electronics with the human body by mimicking the synaptic behaviour of neurons.<sup>136</sup> This form of bioelectronics will greatly facilitate the advancement of human-machine interfaces and interaction. Fig. 10b displays organic electronics that are stretchy, which were made possible by combining an elastomer matrix with an organic semiconducting polymer.<sup>137</sup> These flexible electronics, once constructed, allow for irregular surfaces to interact with soft tissues. The morphology of dielectric materials can be controlled using specialized ways, allowing for lower external energy while improving stretchability in circuits. The absence of power in functional flexible electronics necessitates the use of high-output energy conversion devices. Fig. 10c depicts energy-harvesting flexible electronics constructed from hyper-stretchable elastic composite dielectrics,<sup>138</sup> where the power supply is accomplished by means of the composites' capacity to generate or accumulate energy, following exposure to a specific stimulus. So, whether it is for skin electronics or medical devices, polymer composite dielectrics will surely improve the design of flexible electronics. Nevertheless, it ought to be mentioned that additional efforts are needed to diminish the modulus mismatch among the different materials utilized in nanostructured composites. However, when conducting the experimental design, it is crucial to pay close attention to the composites' homogeneity and structural stability in order to effectively integrate nanoparticles into the polymer matrix.

## 6. Potential applications for scale-up production

Scaling up the production of high-performance polymer nanocomposite dielectrics demands the development of manufacturing platforms that preserve nanoscale dispersion quality, while remaining compatible with industrial throughputs. Emerging strategies such as continuous roll-to-roll solution casting, slot-die coating, and large-scale melt extrusion allow for meter-scale dielectric films to be produced with precise control over thickness, surface morphology, and filler loading. In particular, melt extrusion offers a solvent-free route, making it environmentally and economically attractive for mass production, while surface-modified nanofillers improve the polymer-filler compatibility and prevent aggregation during high-shear processing. Reactive extrusion and *in situ*

nanoparticle synthesis inside polymer matrices are also gaining traction, as they create uniform nanostructures that are difficult to achieve *via* physical blending alone. For multi-layer architectures—such as nanolaminates or gradient-dielectric structures—scale-up involves coextrusion techniques, plasma-assisted deposition, and automated lamination, enabling the integration of multiple dielectric phases with engineered interfaces. As manufacturing expands, quality assurance relies increasingly on inline diagnostics (*e.g.*, optical coherence metrology, capacitance mapping, dielectric spectroscopy) to monitor uniformity and defect density in real time. These scalable production routes directly support demanding applications, including electric vehicle traction inverters, high-voltage DC transmission systems, 5G and future 6G communication modules, aerospace pulsed-power systems, implantable medical electronics, and ultracompact capacitors for flexible and wearable technologies. These fields require dielectric films that can withstand high temperatures, high electric fields, and rapid charge-discharge cycling without significant energy loss. As global electrification accelerates, scaling up polymer nanocomposite dielectrics becomes essential not only for improving device performance, but also for enabling the next generation of lightweight, reliable, and high-energy-density capacitive energy-storage systems.

Dielectric capacitors are perfect for high-performance power electronics and pulsed-power applications because of their high-power density, which means they can quickly absorb and release energy. Pulsed discharge applications need the stored energy to be released within  $10^{-6}$  to  $10^{-3}$  seconds.<sup>139</sup> Medical equipment (such as defibrillators) and surgical lasers are a few examples of potential end users, as are inverters of electricity (an instrument converting DC to AC). In order to detect electrical signals from the heart and administer electric shocks ranging from a few microjoules to severe shocks of 25–40 J in around 5–10 s, implantable cardioverter defibrillators are usually implanted in the chest.<sup>140</sup> Energy densities greater than  $5 \text{ J cm}^{-3}$  are necessary for the capacitors of modern defibrillators.<sup>141</sup> Other uses include electric cars, pulsed weapon systems, and power electronics. Due to the inevitable emergence of pore, void, and microstructural weak spots during large-scale manufacturing, achieving high discharge efficiency in polymer nanocomposite systems has proven to be a formidable issue, particularly when it comes to industrial-scale production. By controlling nanoparticles to build anisotropic nanostructures, the large-scale fabrication of films including nanostructure composites was generated (Fig. 11). Nanocomposites made of this film have a size that can reach  $25 \times 25 \text{ cm}$ . This large-scale production of nanocomposite films achieved an impressively high energy density of  $25.5 \text{ J cm}^{-3}$  and a discharge efficiency of 76.3%.<sup>142</sup> Also, this established technique may be used to produce roll-to-roll processing for large-scale products, which provides opportunities to realizing its practical application. To keep up with the ever-increasing demands in harsh environments, scalable polymer dielectrics targeting increased temperatures are necessary, in addition to room-temperature polymer nanocomposite dielectrics.<sup>141</sup>



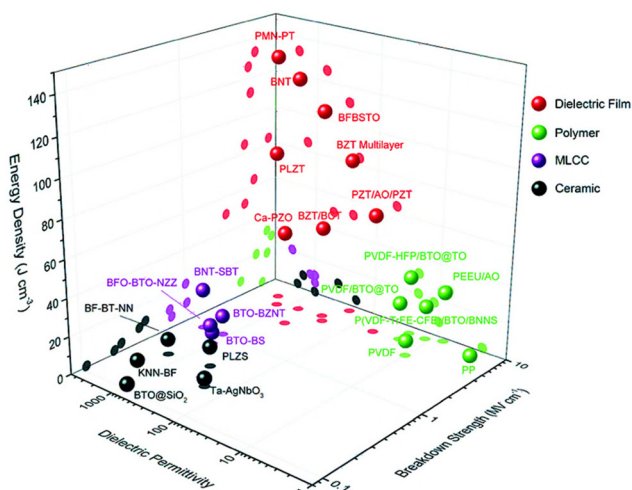


Fig. 11 Summary of the dielectric permittivity versus breakdown strength versus energy density in a 3D plot.<sup>143</sup>

## 7. Conclusions and future outlook

Dielectric capacitors outperform other energy storage materials, such as rechargeable ion batteries, in terms of electrical energy storage owing to its advantages in quick charge/discharge speed, ultrahigh power density, and large cycling life. When subjected to high temperatures, polymer dielectrics exhibit poor charge–discharge efficiency, weak breakdown strength, and low energy density. The negative connection between the two variables means that a neat polymer or ceramic cannot achieve both a high  $E_b$  and  $r$  at the same time. To circumvent the issue of low energy density at high temperatures, the concept of creating a polymer composite dielectric by inserting a ceramic filler into a polymer matrix was put forth.<sup>144</sup> Among polymeric gate dielectrics, materials with a low dielectric constant include poly-4-vinyl phenol, polyvinyl alcohol, and polymethylmethacrylate. There was a notable improvement in the dielectric constant and a decrease in the dielectric loss when inorganic fillers like HfO and TiO<sub>2</sub> were added to the polymer matrix. Yet, the effect of adding nanoparticles depends on how well the nanoparticles mix with the polymer and how evenly they disperse across the network. Luckily, new research on polymer nanocomposite dielectrics has demonstrated that including a trace quantity of inorganic fillers into a polymer matrix can improve electrical characteristics and successfully reduce space charge buildup. We can improve the energy density of polymer nanocomposite dielectrics by adjusting the surface modifier and ceramic filler content to achieve the desired breakdown strength and dielectric characteristic. We created polymer composite dielectrics by mixing h-BN into the polymer matrix. Dielectrics made of polymer composites with h-BN inserted in them have great discharging characteristics at high temperatures and a high energy density because the matrix effectively reduces electrical conduction. Combining BaTiO<sub>3</sub> with a PI matrix resulted in the polymer-based composite dielectrics reaching an impress-

ive energy density of up to 6.0 J cm<sup>-3</sup> at 120 °C and an applied electric field of 200 MV m<sup>-1</sup>.<sup>145</sup> It is of utmost importance to achieve a high charge–discharge efficiency, while obtaining a high energy density at raised temperatures and large applied electric fields. A huge step forward in the development of superior dielectric materials for use at elevated temperatures has been the concept of creating sandwich-structured polymer nanocomposite dielectrics. At the microscopic level, multi-layered structured composites can modify the electric field distribution in polymer composite films. By integrating the merit of each layer, they can simultaneously improve  $U_e$  and  $E_b$ . There have been many studies on polymer composite dielectrics at room temperature—with the goals of high energy density, low dielectric loss, high breakdown strength, and outstanding charge–discharge efficiency—but much less on polymer composite dielectrics operating at high temperatures. Nevertheless, it remains a problem to fabricate a dielectric material with outstanding energy storage capabilities at increased temperatures beyond 150 °C. This review compiles the most up-to-date information on the charge–discharge efficiency and electrical energy storage density of polymer composite dielectrics at raised temperatures and high electric fields in order to show how far this material has come in the last several years. An important aspect of the review is the enhancement of energy density at higher temperatures. This review paper not only has explored methods for enhancing energy density, but has also considered potential avenues for reducing dielectric loss, and achieving high temperature stability and fast-frequency response. We suggest that further development in polymer-based dielectrics should take other application requirements into consideration in order to facilitate industrialization of a wider range of dielectric materials.

Conversely, polymer nanocomposite dielectrics have recently emerged as promising candidates for advanced energy-storage applications because they combine the advantages of polymers—such as high breakdown strength, mechanical flexibility, and ease of processing—with the high dielectric constant of ceramic nanoparticles. Among the different strategies explored, the development of polymer nanocomposites has been the most productive area of research. However, several challenges still limit their practical deployment, including low energy density, long charge–discharge times, limited flexibility, and stability concerns. Critical unresolved issues include the dielectric permittivity mismatch between fillers and the polymer matrix, and the inherent trade-off between achieving high dielectric permittivity and maintaining high breakdown strength. Furthermore, many polymer nanocomposite systems still struggle to attain high discharge efficiency. Addressing these limitations requires new approaches to control and suppress interfacial polarization. Tailoring the local composition and microstructure—through surface modification of fillers, improved dispersion strategies, or designing gradient and multilayer architectures—can significantly mitigate interfacial polarization effects. Effective storage devices also demand sophisticated structural engineering, such as multilayer film construction and optimized series/



parallel configurations, to balance the energy density, breakdown strength, and charge–discharge characteristics. As device complexity increases, current performance evaluation methods based solely on dynamic  $P$ – $E$  loops and static DC analysis become insufficient. Thus, more comprehensive assessment techniques are needed to accurately characterize the dielectric behavior under realistic operating conditions.

Progress in polymer nanocomposite dielectric synthesis and characterization is expected to advance both fundamental material science and the development of high-energy-density storage devices. Ideally, next-generation dielectric materials should possess excellent dielectric properties, high dielectric permittivity, low dissipation factor, superior thermal stability, easy processability, and high mechanical flexibility. Future research must deepen our understanding of filler surface modification, nanoparticle dispersion mechanisms, and the unique properties imparted by nanofillers. Equally important is the discovery of polymer nanocomposites with exceptional thermal stability and high energy density for demanding environments, such as aerospace power systems and subterranean oil exploration. Moreover, insights from advanced computational and simulation models will be crucial for exploring the mechanical, electrical, and interfacial behavior of nanofillers within polymer matrices. For instance, electrical field concentration around high-permittivity nanofillers embedded in low-permittivity polymers can significantly reduce dielectric breakdown strength. Although sandwich-structured nanocomposites have mitigated this issue, a deeper understanding of the mechanisms governing their enhanced performance is still needed.

## Conflicts of interest

The authors declare that there are no competing interests related to this work.

## Data availability

The data used to support the findings of this study are available from the corresponding author upon request.

## References

- H. Li, Y. Zhou, Y. Liu, L. Li, Y. Liu and Q. Wang, *Chem. Soc. Rev.*, 2021, **50**, 6369–6400.
- D. Q. Tan, *Adv. Funct. Mater.*, 2020, **30**, 1808567.
- H. Zhang, T. Wei, Q. Zhang, W. Ma, P. Fan, D. Salamon, S.-T. Zhang, B. Nan, H. Tan and Z.-G. Ye, *J. Mater. Chem. C*, 2020, **8**, 16648–16667.
- B. Liu, M. Yang, W.-Y. Zhou, H.-W. Cai, S.-L. Zhong, M.-S. Zheng and Z.-M. Dang, *Energy Storage Mater.*, 2020, 443–452.
- N. Marati, R. G. Gupta and B. Vaithilingam, *Smart Grid and, Renewable Energy*, IEEE, 2020, pp. 1–6.
- S. Luo, J. Yu, T. Q. Ansari, S. Yu, P. Xu, L. Cao, H. Huang, R. Sun and C.-P. Wong, *Appl. Mater. Today*, 2020, 100882.
- M. Zhang, B. Li, J. J. Wang, H. B. Huang, L. Zhang and L. Q. Chen, *Adv. Mater.*, 2021, 2008198.
- M. Falco, C. Simari, C. Ferrara, J. R. Nair, G. Meligrana, F. Bella, I. Nicotera, P. Mustarelli, M. Winter and C. Gerbaldi, *Langmuir*, 2019, **24**, 8210–8219.
- J. R. Nair, F. Colò, A. Kazzazi, M. Moreno, D. Bresser, R. Lin, F. Bella, G. Meligrana, S. Fantini, E. Simonetti and G. B. Appetecchi, *J. Power Sources*, 2019, **412**, 398–407.
- F. Wu, J. Maier and Y. Yu, *Chem. Soc. Rev.*, 2020, **49**, 1569–1614.
- J. Xie and Q. Zhang, *Small*, 2019, **15**, 1805061.
- S. Li, M. Zhang, Z. Qu, X. Cui, Z. Liu, C. Piao, S. Li, J. Wang and Y. Song, *Chem. Eng. J.*, 2020, **328**, 122394.
- N. G. McCrum, B. E. Read and G. Williams, *Anelastic and Dielectric Effects in Polymeric Solids*, 1967.
- G. Zhang, Q. Li, E. Allahyarov, Y. Li and L. Zhu, *ACS Appl. Mater. Interfaces*, 2021, **13**, 37939–37960.
- Z. Ahmad, *Polymer dielectric materials*, IntechOpen, 2012.
- S. Wenjie, M. Jiale, W. Shuang, L. Zhang and Y. Cheng, *Front. Chem. Sci. Eng.*, 2021, **15**, 18–34.
- N. Guo, S. A. DiBenedetto, P. Tewari, M. T. Lanagan, M. A. Ratner and T. J. Marks, *Chem. Mater.*, 2010, **23**, 1567–1578.
- Z.-H. Dai, T. Li, Y. Gao, J. Xu, J. He, Y. Weng and B.-H. Guo, *Compos. Sci. Technol.*, 2019, **169**, 142–150.
- Y. Zhang, C. Zhang, Y. Feng, T. Zhang, Q. Chen, Q. Chi, L. Liu, G. Li, Y. Cui, X. Wang, Z. Dan and Q. Lei, *Nano Energy*, 2019, **56**, 138–150.
- S. Guan, H. Li, S. Zhao and L. Guo, *Compos. Sci. Technol.*, 2018, **12**, 79–85.
- X. Huang, B. Sun, Y. Zhu, S. Li and P. Jiang, *Prog. Mater. Sci.*, 2019, **1**, 187–225.
- W. Li, Q. Meng, Y. Zheng, Z. Zhang, W. Xia and Z. Xu, *Appl. Phys. Lett.*, 2010, **96**, 19.
- W. Xia and Z. Zhang, *Nanodielectrics*, 2018, **1**, 17–31.
- B. L. Farmer, A. J. Hopfinger and J. B. Lando, *J. Appl. Phys.*, 1972, 43.
- V. Bharti, X. Z. Zhao, Q. M. Zhang, T. Romotowski, F. Tito and R. Ting, *Mater. Res. Innovations*, 1998, **2**, 57–63.
- H. Xu, G. Shanthi, V. Bharti, Q. M. Zhang and T. Ramotowski, *Macromolecules*, 2000, **33**, 4125–4131.
- M. R. Gadinski, C. Chanthad, K. Han, L. Dong and Q. Wang, *Polym. Chem.*, 2014, **5**, 5957–5966.
- Y. Zhang, C. Zhang, Y. Feng, T. Zhang, Q. Chen, Q. Chi, L. Liu, X. Wang and Q. Lei, *Nano Energy*, 2019, **66**, 104–195.
- Y. Zhang, Q. Chi, L. Liu, C. Zhang, C. Chen, X. Wang and Q. Lei, *APL Mater.*, 2017, **5**, 7.
- P. Prabhune, Y. Comlek, A. Shandilya, R. Sundararaman, L. S. Schadler, L. C. Brinson and Chew, *Nanomaterials*, 2023, **22**, 2394.
- Y. Hao, X. Wang, K. Bi, J. Zhang, Y. Huang, L. Wu, P. Zhao, K. Xu, M. Lei and L. Li, *Nano Energy*, 2017, **31**, 49–56.



- 32 K. Bi, M. Bi, Y. Hao, W. Luo, Z. Cai, X. Wang and Y. Huang, *Nano Energy*, 2018, **51**, 513–523.
- 33 P. Wu, L. Zhang and X. Shan, *Mater. Lett.*, 2015, **159**, 72–75.
- 34 L. Yao, Z. Pan, J. Zhai, G. Zhang, Z. Liu and Y. Liu, *Appl. Sci. Manuf.*, 2018, **109**, 48–54.
- 35 Y. Bai, Z. Y. Cheng, V. Bharti, H. Xu and M. Zhang, *Appl. Phys. Lett.*, 2000, **76**, 3804–3806.
- 36 S. Wang, J. Sun, L. Tong, Y. Guo, H. Wang and C. Wang, *Mater. Lett.*, 2018, **211**, 114–117.
- 37 X. Lu, L. Zhang, Y. Tong and Z. Cheng, *Composites, Part B*, 2019, **168**, 34–43.
- 38 H. Sun, H. Zhang, S. Liu, N. Ning, L. Zhang, M. Tian and Y. Wang, *Compos. Sci. Technol.*, 2018, **154**, 145–153.
- 39 Q. Wang and L. Zhu, *J. Polym. Sci., Part B: Polym. Phys.*, 2011, **49**, 1421–1429.
- 40 T. Tanaka, M. Kozako, N. Fuse and Y. Ohki, *IEEE Trans. Dielectr. Electr. Insul.*, 2005, **12**, 669–681.
- 41 T. J. Lewis, *J. Phys. D: Appl. Phys.*, 2005, **3**, 202.
- 42 A. Yializis and R. S. Taylor, InDoE Annual Merit Review Meeting 2017, 6.
- 43 X. Zhang, J. Jiang, Z. Shen, Z. Dan, M. Li, Y. Lin, C. W. Nan, L. Chen and Y. Shen, *Adv. Mater.*, 2018, **30**, 170.
- 44 B. Zaarour, L. Zhu, C. Huang and X. Jin, *Polym. Adv. Technol.*, 2021, **33**, 1449–1462.
- 45 F. Ran, T. Wang, S. Chen, Y. Liu and L. Shao, *Appl. Surf. Sci.*, 2020, **511**, 42.
- 46 L. Chen, S. Wang, Q. Yu, P. D. Topham, C. Chen and L. Wang, *Soft Matter*, 2019, **15**, 2490–2510.
- 47 M. J. C. Nalbandian, Development and optimization of chemically-active electrospun nanofibers for treatment of impaired water sources, University of California, Riverside, 2014.
- 48 B. Henriques, P. Pinto, J. Souza, J. C. Teixeira, D. Soares and F. S. Silva, *Gold Bull.*, 2013, **46**, 117–125.
- 49 R. Chokshi and H. Zia, *Iran. J. Pharm. Res.*, 2004, **3**, 3–16.
- 50 D. Franla, C. K. Jen, K. Nguyen and R. Gendron, *Polym. Eng. Sci.*, 2000, **40**, 82–94.
- 51 K. Lamnawar and A. Maazouz, *Polym. Eng. Sci.*, 2009, **49**, 727–739.
- 52 J. Xiong, X. Wang, X. Zhang, Y. Xie, J. Lu and Z. Zhang, *J. Appl. Polym. Sci.*, 2021, **138**, 50029.
- 53 Z. Xie, D. Liu, K. Wu and Q. Fu, *Polymer*, 2021, **214**, 123348.
- 54 S. A. R. Daniel and Qi Tan, *High Performance DC Bus Film Capacitor*, 2015, pp. 221–232.
- 55 D. Langhe, L. Zhu, M. Brubaker and L. Marlino, *Polymer*, Plus LLC, Valley View, OH (United States), 2017.
- 56 X. Chen, E. Allahyarov, D. Langhe, M. Ponting, R. Li, M. Fukuto, D. E. Schuele, E. Baer and L. Zhu, *J. Mater. Chem. C*, 2020, **18**, 6102–6117.
- 57 <https://www.tri-cor.com/how-polyethylene-film-is-made/#:~:text=This%20plastic%20film%20manufacturing%20process,they%20become%20molten%20and%20pliable.&text=The%20molten%20plastic%20is%20pushed,of%20plastic%20called%20the%20bubble>, in. 2021.
- 58 J. Xiong, X. Wang, X. Zhang, Y. Xie, J. Lu and Z. Zhang, *J. Appl. Polym. Sci.*, 2021, **15**, 50029.
- 59 J. Jiang, Z. Shen, X. Cai, J. Qian, Z. Dan and Y. Lin, *Adv. Energy Mater.*, 2019, **9**, 1–9.
- 60 H. Hu, F. Zhang, S. Lim, P. Blanloeuil, Y. Yao, Y. Guo and C. H. Wang, *Composites, Part B*, 2019, **178**, 107459.
- 61 Q. Li, F.-Z. Yao, Y. Liu, G. Zhang, H. Wang and Q. Wang, *Annu. Rev. Mater. Res.*, 2018, **48**, 219–243.
- 62 J. Yang, Z. Tang, H. Yin, Y. Liu, L. Wang and L. Y. Tang, *Polymers*, 2019, **11**, 766.
- 63 S. Zhang, C. Zou, D. I. Kushner, X. Zhou, R. J. Orchard, N. Zhang and Q. M. Zhang, *IEEE Trans Dielectr. Electr. Insul.*, 2012, **19**, 1158–1166.
- 64 Y. Wang, J. Cui, Q. Yuan, Y. Niu, Y. Bai and H. Wang, *Adv. Mater.*, 2015, **27**, 6658.
- 65 Q. Li, F. Liu, T. Yang, M. R. Gadinski, G. Zhang, L. Q. Chen and Q. Wang, *Proc. Natl. Acad. Sci. U. S. A.*, 2016, **113**, 9995.
- 66 Z. H. Shen, J. J. Wang, Y. Lin, C. W. Nan, L. Q. Chen and Y. Shen, *Adv. Mater.*, 2018, **30**, 1704380.
- 67 University of Cambridge. TLP Library Dielectric materials – Loss in dielectrics. <https://www.doitpoms.ac.uk/tlplib/dielectrics/loss.php>, 2020.
- 68 W. Xu, J. Liu, T. Chen, X. Jiang, X. Qian, Y. Zhang, Z. Jiang and Y. Zhang, *Small*, 2019, **15**, 1–8.
- 69 H. Palneedi, M. Peddigari, G. T. Hwang, J. Dy and J. Ryu, *Adv. Funct. Mater.*, 2018, **28**, 1–33.
- 70 Z. Wang, N. M. Han, Y. Wu, X. Liu, X. Shen, Q. Zheng and J.-K. Kim, *Carbon*, 2017, **123**, 385.
- 71 N. M. D. P. Kim, J. P. Tillotson, P. J. Hotchkiss, M.-J. Pan, S. R. Marder, J. Li, J. P. Calame and J. W. Perry, *ACS Nano*, 2009, **3**, 2581.
- 72 Y. Niu, F. Xiang, Y. Wang, J. Chen and H. Wang, *Phys. Chem. Chem. Phys.*, 2018, **20**, 6598.
- 73 Z.-H. Dai, T. Li, Y. Gao, J. Xu, Y. Weng, J. He and B.-H. Guo, *Colloids Surf., A*, 2018, **548**, 179.
- 74 J. Fu, Y. Hou, M. Zheng, Q. Wei, M. Zhu and H. Yan, *ACS Appl. Mater. Interfaces*, 2015, **7**(7), 24480.
- 75 K. Yu, H. Wang, Y. Zhou, Y. Bai and Y. Niu, *J. Appl. Phys.*, 2013, **113**, 1034105.
- 76 K. Yu, Y. Niu, F. Xiang, Y. Zhou, Y. Bai and H. Wang, *J. Appl. Phys.*, 2013, **114**, 174107.
- 77 H. Luo, D. Zhang, C. Jiang, X. Yuan, C. Chen and K. Zhou, *ACS Appl. Mater. Interfaces*, 2015, **7**, 8061.
- 78 P. Hu, S. Gao, Y. Zhang, L. Zhang and C. Wang, *Compos. Sci. Technol.*, 2018, **156**, 109.
- 79 K. Yu, Y. Niu, Y. Zhou, Y. Bai, H. Wang and C. Randall, *J. Am. Ceram. Soc.*, 2013, **96**, 2519.
- 80 S. Liu and J. Zhai, *J. Mater. Chem. A*, 2015, **3**, 1511.
- 81 G. Wang, X. Huang and P. Jiang, *ACS Appl. Mater. Interfaces*, 2017, **9**, 7547.
- 82 H. Tang and H. A. Sodano, *Nano Lett.*, 2013, **13**, 1373.
- 83 H. Tang, Y. Lin and H. A. Sodano, *Adv. Energy Mater.*, 2013, **3**, 451.
- 84 H. Luo, Z. Wu, X. Zhou, Z. Yan, K. Zhou and D. Zhang, *Compos. Sci. Technol.*, 2018, **106**, 237.



- 85 L. Gao, J. He, J. Hu and Y. Li, *J. Phys. Chem. C*, 2014, **118**, 831.
- 86 H.-J. Ye, W.-Z. Shao and L. Zhen, *Colloids Surf., A*, 2013, **427**, 19.
- 87 Y. Kim, O. N. L. Smith, M. Kathaperumal, L. R. Johnstone, M.-J. Pan and J. W. Perry, *RSC Adv.*, 2014, **4**, 19668.
- 88 K. Yang, X. Huang, Y. Huang, L. Xie and P. Jiang, *Chem. Mater.*, 2013, **25**, 2327.
- 89 S. Liu, S. Xue, W. Zhang and J. Zhai, *Ceram. Int.*, 2014, **40**, 15633.
- 90 P. Hu, Y. Song, H. Liu, Y. Shen, Y. Lin and C.-W. Nan, *J. Mater. Chem. A*, 2013, **1**, 1688.
- 91 Y. Wu, Z. Wang, X. Shen, X. Liu, N. M. Han, Q. Zheng, Y. W. Mai and J. K. Kim, *ACS Appl. Mater. Interfaces*, 2018, **10**, 26641.
- 92 J. Kammermaier, *IEEE Trans. Electr. Insul.*, 1987, **22**, 145–149.
- 93 L. Zhao, J. Sun and Q. Fang, *Polym. Chem.*, 2024, **15**, 3063.
- 94 J. Hou, J. Sun and Q. Fang, *Polym. Chem.*, 2023, **14**, 3203.
- 95 L. Li, W. Xu, G. Rui, S. Zhang, Q. M. Zhang and Q. Wang, *Chem. Sci.*, 2024, **15**, 19651–19668.
- 96 Y. Shen and C.-W. Nan, *Natl. Sci. Rev.*, 2023, **11**, 224.
- 97 H. Aldosari, N. Madkhali, S. Algasser and M. Khairy, *Curr. Nanomater.*, 2024, **9**, 367–376.
- 98 Z. Fan, B. Li, D. Ren and M. Xu, *Polymers*, 2023, **15**, 3933.
- 99 J. Ho and T. R. Jow, *IEEE Trans. Dielectr. Electr. Insul.*, 2012, **19**, 990–995.
- 100 N. Zebouchi, M. Bendaoud, R. Essolbi, D. Malec, B. Ai and H. Giam, *J. Appl. Phys.*, 1996, **79**, 2497–2501.
- 101 Prateek, V. K. Thakur and R. K. Gupta, *Chem. Rev.*, 2016, **116**, 4260–4317.
- 102 Q. Li, G. Zhang, F. Liu, K. Han, M. R. Gadinski, C. X. Xiong and Q. Wang, *Energy Environ. Sci.*, 2015, **8**, 922–993.
- 103 J. Jiang, Z. Shen, J. Qian, Z. Dan, M. Guo, Y. Lin, C. Nan, L. Chen and Y. Shen, *Energy Storage Mater.*, 2019, **18**, 213–221.
- 104 S. Chen, G. Meng, B. Kong, B. Xiao, Z. Wang, Z. Jing, Y. Gao, G. Wu, H. Wang and Y. Cheng, *Chem. Eng. J.*, 2020, **387**, 123662.
- 105 F. Guan, J. Wang, L. Yang, J. Tseng, K. Han, Q. Wang and L. Zhu, *Macromolecules*, 2011, **44**, 2190–2199.
- 106 F. Guan, Z. Yuan, E. W. Shu and L. Zhu, *Appl. Phys. Lett.*, 2009, **94**, 052907.
- 107 P. Prabhune, Y. Comlek, A. Shandilya, R. Sundararaman, L. S. Schadler, L. C. Brinson and W. Chen, *Nanomaterials*, 2003, **13**, 2394.
- 108 J. Fothergill, *IEEE Trans. Electr. Insul.*, 1991, **26**, 1124–1129.
- 109 X. Wu, S. Tang, G. Song, Z. Zhang and D. Q. Tan, *Nano*, 2021, **2**, 10025.
- 110 X. Li, B. Liu, J. Wang, S. Li, X. Zhen, J. Zhi, J. Zou, B. Li, Z. Shen, X. Zhang and S. Zhang, *Nat. Commun.*, 2024, **15**, 51052.
- 111 Q. Li, L. Chen, M. R. Gadinski, S. Zhang, G. Zhang, H. U. Li, E. Iagodkine, A. Haque, L.-Q. Chen and T. N. Jackson, *Nature*, 2015, **523**, 576–579.
- 112 Q. Burlingame, S. Wu, M. Lin and Q. Zhang, *Adv. Energy Mater.*, 2013, **3**, 1051–1055.
- 113 M. Singh, P. Das, P. N. Samanta, S. Bera, R. Thanirige, B. Shook, R. Nejat, B. Behera, Q. Zhang, Q. Dai and A. Pramanik, *ACS Nano*, 2023, **17**, 12482–12491.
- 114 J. Ding, W. Xu, X. Zhu, Z. Liu, Y. Zhang and Z. Jiang, *Nano Res.*, 2003, **16**, 5813–5823.
- 115 H. Li, Y. Zhou, Y. Liu, L. Li, Y. Liu and Q. Wang, *Chem. Soc. Rev.*, 2021, **50**(11), 6369–6400.
- 116 M. Yang, M. Guo, E. Xu, W. Ren, D. Wang, S. Li, S. Zhang, C. W. Nan and Y. Shen, *Nat. Nanotechnol.*, 2024, **19**, 588–603.
- 117 M. E. Kennedy and D. L. Hollenbaugh Jr, inventors; Gore Enterprise Holdings Inc, assignee. Fluoropolymer barrier material, United States patent US 7521010, 2009.
- 118 Q. Li, F. Z. Yao, Y. Liu, G. Zhang, H. Wang and Q. Wang, *Annu. Rev. Mater. Res.*, 2018, **47**, 219–243.
- 119 Q. Li, L. Chen, M. R. Gadinski, S. Zhang, G. Zhang, H. Li, E. Iagodkine, A. Haque, L. Chen, T. Jackson and Q. Wang, *Nature*, 2015, **523**, 576–579.
- 120 T. R. Jow, F. W. MacDougall, J. B. Ennis, X. H. Yang, M. A. Schneider, C. J. Scozzie, J. D. White, J. R. MacDonald, M. C. Schalnath, R. A. Cooper and S. P. Yen, Pulsed power capacitor development and outlook, in *2015 IEEE Pulsed Power Conference (PPC)*, IEEE, 2015, pp. 1–7.
- 121 C. Lynn, A. Neuber, E. Matthews, J. Walter and M. Kristiansen, A low impedance 500kV 2.7 kJ Marx generator as testbed for vacuum diodes, in *2010 IEEE International Power Modulator and High Voltage Conference*, IEEE, 2010, pp. 417–420.
- 122 V. A. Stephanovich, I. A. Luk'yanchuk and M. G. Karkut, *Phys. Rev. Lett.*, 2005, **94**, 47601.
- 123 B. Chu, X. Zhou, K. Ren, B. Neese, M. Lin, Q. Wang, F. Bauer and M. Zhang, *Science*, 2006, **313**, 334–336.
- 124 [https://blogger.googleusercontent.com/img/b/R29vZ2xl/AVvXsEir67Ab3BaAw9Xn7RcqP289y5dvel9jHMXpS902KKfsoYGXJ8ZA1cAL\\_FqCr476QMaXcBGMARXHWwFwWFI0Hps2ZxVwwACsFvA\\_hZsS0WwHNxe8zHWYTYzMGt1PlyqjnDkrP-nd0/s750/MARX-Generator.png](https://blogger.googleusercontent.com/img/b/R29vZ2xl/AVvXsEir67Ab3BaAw9Xn7RcqP289y5dvel9jHMXpS902KKfsoYGXJ8ZA1cAL_FqCr476QMaXcBGMARXHWwFwWFI0Hps2ZxVwwACsFvA_hZsS0WwHNxe8zHWYTYzMGt1PlyqjnDkrP-nd0/s750/MARX-Generator.png).
- 125 R. J. Young and P. A. Lovell, *Introduction to polymers*, CRC press, 2011.
- 126 E. Baer and L. Zhu, *Macromolecules*, 2017, **50**(6), 2239–2256.
- 127 R. Yang, R. Wei, K. Li, L. Tong, K. Jia and X. Liu, *Sci. Rep.*, 2016, 36434.
- 128 N. Venkat, T. D. Dang, Z. Bai, V. K. McNier, J. N. DeCerbo, B. H. Tsao and J. T. Stricker, *Mater. Sci. Eng., B*, 2010, **168**, 16–21.
- 129 J. Pan, K. Li, S. Chuayprakong, T. Hsu and Q. Wang, *ACS Appl. Mater. Interfaces*, 2010, **2**, 286–289.
- 130 Q. Li, F. Z. Yao, Y. Liu, G. Zhang, H. Wang and Q. Wang, *Annu. Rev. Mater. Res.*, 2018, **48**, 219–243.
- 131 B. Wang, W. Huang, L. Chi, M. Al-Hashimi, T. J. Marks and A. Facchetti, *Chem. Rev.*, 2018, **118**, 5690.
- 132 M. D. Bartlett, A. Fassler, N. Kazem, E. J. Markvicka, P. Mandal and C. Majidi, *Adv. Mater.*, 2016, **28**, 3726.



- 133 C. Lu, W. Y. Lee, C. C. Shih, M. Y. Wen and W. C. Chen, *ACS Appl. Mater. Interfaces*, 2017, **9**, 25522.
- 134 Z. Liu, Z. Yin, S.-C. Chen, S. Dai, J. Huang and Q. Zheng, *Org. Electron.*, 2018, **53**, 205.
- 135 Y. J. Tan, H. Godaba, G. Chen, S. T. M. Tan, G. Wan, G. Li, P. M. Lee, Y. Cai, S. Li, R. F. Shepherd, J. S. Ho and B. C. K. Tee, *Nat. Mater.*, 2020, **19**, 182.
- 136 F. Molina-Lopez, T. Z. Gao, U. Kraft, C. Zhu, T. Ohlund, R. Pfattner, V. R. Feig, Y. Kim, S. Wang, Y. Yun and Z. Bao, *Nat. Commun.*, 2019, **10**, 2676.
- 137 R. Ma, S. Y. Chou, Y. Xie and Q. Pei, *Chem. Soc. Rev.*, 2019, **48**, 1741.
- 138 <https://scx1.b-cdn.net/csz/news/800a/2015/akaistresear.jpg>.
- 139 T. R. Jow, F. W. MacDougall, J. B. Ennis, X. H. Yang, M. A. Schneider, C. J. Scozzie, J. D. White, J. R. Mac Donald, M. C. Schalnat, R. A. Cooper and S. P. S. Yen, Pulsed power capacitor development and outlook, in *2015 IEEE Pulsed Power Conference (PPC)*, IEEE, 2015, vol. 1.
- 140 A. M. Crespi, S. K. Somdahl, C. L. Schnidt and P. M. Skarstad, *J. Power Sources*, 2001, **96**, 33.
- 141 A. Braga and R. Cooper, *Anaesthesiol. Intensive Care Med.*, 2018, **19**, 329.
- 142 X. Zhang, J. Jiang, Z. Shen, Z. Dan, M. Li, Y. Lin, C. W. Nan, L. Chen and Y. Shen, *Adv. Mater.*, 2018, **30**, 1707269.
- 143 H. Pan, A. Kursumovic, Y.-H. Lin, C.-W. Nan and J. L. MacManus-Driscoll, *Nanoscale*, 2020, **12**, 19582–19591.
- 144 Q. Li, L. Chen, M. R. Gadinski, S. Zhang, G. Zhang and H. Li, *Nature*, 2015, **523**, 576–579.
- 145 M. Rajib, R. Martinez, M. Shuvo, H. Karim, D. Delfin and S. Afrin, *Int. J. Appl. Ceram. Technol.*, 2016, **13**, 125–132.

